Abstracts, Division of Biological Chemistry, 203rd National Meeting of the American Chemical Society, April 5–10, 1992

Perry A. Frey, Chair; George L. Kenyon, Chair Elect;
Judith P. Klinman, Program Chair; Gregory Petsko, Program Chair Elect

1. Localized Mutagenesis of Protein and Substrate in the Isocitrate Dehydrogenase Reaction. *Daniel E. Koshland, Jr.*, Barry Stoddard, Myoung Lee, and Antony Dean. Department of Molecular and Cell Biology, University of California, Berkeley, CA 94720.

The three-dimensional structure and much of the mechanism of action of isocitrate dehydrogenase has been revealed by X-ray crystallography and kinetic analysis. Oxalosuccinate is found not to be an intermediate by kinetic analysis, although both its decarboxylation and reduction are catalyzed by the enzyme. The metal ion, Mg^{2+}, is positioned at precisely the position expected from the Sternberger–Westheimer organic model for decarboxylations. The substitution of other divalent metals for Mg introduces changes in rates that indicate subtle interactions between metal ions, substrate, and protein conformation. The ease of modifying both the substrate and the protein has made it possible to explore the interactions of the active site in unusual ways to modify specificity and catalytic action.

2. Phospholipase A_2 Structure, Mechanism, and Role in Signal Transduction. *Edward A. Dennis* and Lin Yu. Department of Chemistry, 0601, University of California at San Diego, La Jolla, CA 92093-0601.

Phospholipase A_2 (PLA_2) catalyzes the hydrolytic release of the fatty acid at the *sn*-2 position of membrane lipids. It plays a central role in the production of lipid second messengers in signal transduction as its products are free arachidonic acid and lysophospholipids; these are also precursors of the prostaglandins and platelet activating factor (PAF). We have recently solved the X-ray crystal structure of the PLA_2 from cobra venom (*Naja naja naja*), which contains 119 amino acids and 7 disulfide bonds. Studies of the mechanism of action of the enzyme at the lipid–water interface have relied on substrate analogues, which serve as inhibitors. Thioether amide analogues bind as much as 10^4 tighter than normal phospholipids. Recent pH-dependent studies show that the amides bind to the neutral form of His-48 at the catalytic site. In contrast, thioether phosphonates bind to the protonated form. Thus amides are more potent inhibitors than phosphonates at the optimal pH of the enzyme [Yu & Dennis (1991) *Proc. Natl. Acad. Sci. U.S.A. 88*, 9325]. Recent studies with a variety of thioether amide phospholipids of various acyl chain lengths as monomers, micelles, and mixed micelles help elucidate and define the catalytic site and mechanism of action further.

3. Mandelate Racemase: Understanding the Mechanism of Heterolytic C–H Bond Cleavage. *J. A. Gerlt*,[1] G. L. Kenyon,[2] J. W. Kozarich,[1] D. J. Neidhart,[3] and G. A. Petsko.[4] [1]University of Maryland, College Park, MD 20742, [2]University of California, San Francisco, CA 94143, [3]Abbott Laboratories, Abbott Park, IL 60064, and [4]Brandeis University, Waltham, MA 02254.

The mechanism of the reaction catalyzed by mandelate racemase has been examined by the combined approaches of site-directed mutagenesis, chemical modification, and X-ray crystallography. The enantiomers of mandelate are interconverted by the participation of two acid/base catalysts directly involved in C–H bond cleavage (Lys-166 and His-297). In addition, Lys-164, Glu-317, and the essential Mg^{2+} interact with the carboxylate group of the substrate to facilitate formation of an enolate intermediate, thereby allowing the rapid rates of the proton-transfer reactions to be understood. (Supported by NIH GM-40570.)

4. Evolutionary Guidance in Biological Chemistry. *Steven A. Benner*. Laboratory for Organic Chemistry, ETH, Zurich, CH-8092 Switzerland.

The rational manipulation of protein structure requires accurate models describing how proteins evolve. Evolutionarily tools based on these models that have been developed recently at ETH include (a) Computer programs that permit "all-against-all matching" of the protein sequence database, yielding reliable scores for mutations and deletions, reconstructed ancient protein sequences, and models of ancient metabolisms. (b) Comprehensive models describing the selection of kinetic, stereochemical, and physical behavior in enzymes. (c) Accurate methods for predicting de novo the folded structure of proteins without crystallographic data. (d) An expanded genetic alphabet and genetic lexicon, where additional nucleic acid base pairs yield additional triplet codons, increasing the number of types of amino acids that can be built into proteins by translation. These tools have enabled the following contributions: (a) Genes for ancient enzymes dating back ca. 500 million years have been prepared and expressed in a physiologically relevant host where subsequent in vivo evolution of the ancient protein can be followed. (b) Peptides have been designed that fold in aqueous solution (with structure proven by NMR) and catalyze reactions (with rate enhancements and mechanisms accurately established by physical organic methods). (c) Nucleic acids analogues with sulfone groups instead of phosphates have been prepared. These bind complementary nucleic acid, are stable to hydrolysis, and pass across biological barriers. Through the use of these tools, it has been possible to discover a new and unanticipated class of growth regulators in higher organisms: extracellular RNases and RNA. The story of this discovery will be related.

5. The Westheimer Research Group—Recollections. *F. H. Westheimer*. Department of Chemistry, Harvard University, 12 Oxford Street, Cambridge, MA 02138.

0006-2960/92/0431-2188$03.00/0

Recollections of challenging chemical research and of great collaborators who worked with me over the course of almost 60 years at the University of Chicago and at Harvard will be presented.

6. Functional Significance of Intersubunit Electrostatic Interactions at the Active Site of *R. rubrum* Ribulose-bisphosphate (RuBP) Carboxylase/Oxygenase. Mark R. Harpel, Frank W. Larimer, Eva H. Lee, Richard J. Mural, Thomas S. Soper, and *Fred C. Hartman.* Biology Division, Oak Ridge National Laboratory, Oak Ridge, TN 37831.

The active site of the enzyme consists of residues from the large β/α barrel domain of one subunit and from the small N-terminal domain of the adjacent subunit. The nonactivated form of the enzyme contains an intersubunit, electrostatic interaction between active-site residues Glu48 and Lys168. Ligand binding to the activated form of the enzyme immobilizes a flexible loop of the β/α barrel, resulting in formation of a new, intersubunit salt bridge between Glu48 and active-site Lys329 [Knight et al. (1990) *J. Mol. Biol. 215*, 113; Schneider et al. (1990) *J. Mol. Biol. 211*, 989]. Site-directed mutagenesis shows that neither salt bridge is necessary for proper subunit association and that the constituent side chains are not required for enzyme activation, substrate binding, or enolization of RuBP (the initial catalytic event). Each of the three side chains is, however, crucial to later stages of the overall reaction pathway. Mutant characterization, including application of chemical rescue [Toney and Kirsch (1990) *Science 243*, 1485], also demonstrates the importance of Glu48 and Lys329 in proper discrimination of the two gaseous substrates. (ORNL is managed by Martin Marietta Energy Systems, Inc., under Contract DE-AC05-84OR21400 with the U.S. Department of Energy.)

7. Conversion of Arg292 of *E. coli* Aspartate Aminotransferase to Homoarginine and Introduction of Negative Cooperativity by the D222A Mutation. *Jack F. Kirsch*, Peter W. White, and James J. Onuffer. Molecular and Cell Biology Department, Barker Hall, University of California, Berkeley, CA 94720.

The side chain of Arg292 of the title enzyme has been converted to homoarginine by treatment of the R292K mutant with *O*-methylisourea. Enzyme activity, which is reduced by 3–4 orders of magnitude from wild type in the R292K mutant, is increased several hundredfold following the chemical modification step. Asp222, which hydrogen bonds to the pyridinium nitrogen atom of pyridoxal phosphate, has been converted to alanine (D222A). This enzyme form exhibits $\sim 10^{-4}$ of the activity of wild-type enzyme. It also shows nonhyberbolic saturation behavior in its kinetics with amino acid substrates which are indicative of negative cooperativity. Detailed steady-state and single-turnover kinetic analyses of heterodimer constructs containing the D222A mutant in one subunit show that the negative cooperativity is the result of two slowly interconverting enzyme forms.

8. Mutagenesis with Unnatural Amino Acids. *P. G. Schultz.* Department of Chemistry, University of California, Berkeley, CA 94720.

A general biosynthetic method has been developed which makes it possible to site-specifically incorporate unnatural amino acids with novel steric and electronic properties into proteins. The approach involves replacement of the codon encoding the amino acid of interest with the "blank" nonsense codon, TAG, by oligonucleotide-directed mutagenesis. A suppressor tRNA directed against this unique codon is then chemically or genetically generated and chemically aminoacylated in vitro with the desired unnatural amino acid. Addition of the aminoacylated tRNA to an in vitro protein-synthesizing system programmed with the mutagenized DNA directs the unique insertion of the prescribed amino acid into the protein at the target site. This methodology has recently been applied to a number of proteins including *ras* oncogene product, T4 lysozyme, and 434 repressor. The catalytic properties, specificity, and stability of these proteins have been studied by substituting amino acids with altered pK_a's and nucleophilicities, restricted conformations, altered redox and steric properties, as well as photoactivable and photocleavable amino acids.

9. Spectral Studies of the Active Site Mutants, C44S and C49S, of *Escherichia coli* Lipoamide Dehydrogenase. N. Hopkins and *C. H. Williams, Jr.* Department of Biological Chemistry, University of Michigan and VA Medical Center, Ann Arbor, MI 48105.

E. coli lipoamide dehydrogenase, a dimeric flavoprotein, is a member of the pyridine nucleotide–disulfide oxidoreductase family. The enzyme catalyzes the reduction of NAD^+ by dihydrolipoamide. The two cysteine residues which comprise the redox active disulfide/dithiol are Cys-44 and Cys-49. Cys-44 interchanges with the dithiol substrate and Cys-49 interacts with the FAD. The mutations changing each Cys to a Ser (C44S, C49S) have been characterized. Reductive titrations using NADH have shown that the flavin of C44S is more difficult to reduce than that of C49S. Titrations of C44S using dithionite as the reductant from pH 4.8 to 8.9 indicated that the reduced flavin existed in two protonic forms, $FADH_2$ and $FADH^-$ with a pK_a of 7.9. Reoxidation of the enzyme with NAD^+ was stoichiometric at pH values above 7.6, while at pH values below 7.6 excess NAD^+ was required. In contrast, titrations of C49S using dithionite as the reductant and NAD^+ as the (re)oxidant at pH 7.6 required an excess of NAD^+, and full reoxidation was not attainable. These experiments resulted in estimated redox potentials at pH 7.6, 20 °C of −321 mV for C49S and −356 mV for C44S. (Supported by the Health Services and Research Administration of the Department of Veterans Affairs and by Grant GM21444 from the N.I.G.M.S. N.H. is supported by a Rackham Minority Merit Fellowship from the Graduate School at the University of Michigan.)

10. Functional Single and Multiple Site Mutations in the Heme Environment of Iso-1 Cytochrome *c*. Sonja Komar-Panicucci and *George L. McLendon.* Department of Chemistry, University of Rochester, Rochester, NY 14627.

A series of functional single and multiple site mutations in the heme environment of *Saccharomyces cerevisiae* iso-1 cytochrome *c* have been made by site-directed mutagenesis. We have measured the formal redox potentials of the resultant proteins and have observed shifts, relative to the wild-type protein, as large as 115 mV. Chemical denaturation of the proteins indicates that some mutants are more stable than the native structure. The results of these studies are being used to address the question of control of the redox potential of cytochrome *c* and to address the question of additive effects from multiple mutation sites in cytochrome *c*.

11. An Integrated Approach to Drug Design Involving Synthesis, NMR Spectroscopy, and Computer Simulations.

Murray Goodman. Department of Chemistry, 0343, University of California, San Diego, La Jolla, CA 92093-0343.

The physiological effects of brain peptides are revealed by stereospecific binding to their receptors. To understand the molecular basis of receptor-mediated physiological phenomena, it is necessary to have highly selective ligands and to explore their conformational features. Our laboratories have investigated such ligands for several receptor systems and elucidated structure–bioactivity relationships through an integrated approach including synthesis, bioassays, NMR spectroscopy, and computer simulations. Many of the peptides and peptidomimetics synthesized in our laboratories have exhibited high potency, selectivity, and enzymatic stability. Also, the conformational studies of these molecules have led to the development of topochemical models for bioactivity of opioids, somatostatins, neuropeptides, peptide antibiotics, and taste ligands. This lecture will focus on our achievements in the opioid and somatostatin area. We have designed and synthesized many novel opioids and somatostatins by incorporating peptidomimetics such as retro-inverso modifications, constrained amino acids, and cyclic structures. We have developed general models which can be applied for all the families of peptide opioids and somatostatins.

12. Designing Zinc Finger Proteins. *Jeremy M. Berg.* Department of Biophysics and Biophysical Chemistry, The Johns Hopkins University School of Medicine, Baltimore, MD 21205.

Zinc finger proteins are a family of specific DNA binding proteins characterized by the presence of sequences of the form (Tyr,Phe)-X-Cys-$X_{2,4}$-Cys-X_3-Phe-X_5-Leu-X_2-His-$X_{3,4}$-His-X_5, usually in tandem arrays. Each of these sequences binds a zinc (or other metal) ion via the invariant Cys and His residues. Structural studies have revealed that each of the sequences folds to form a domain consisting of two β strands followed by a helix and that the helix plays the major role in site-specific DNA binding. A variety of novel zinc finger domains and proteins have been designed and synthesized to probe structural, metal ion binding specificity, and DNA binding recognition determinants. Studies of these materials by a variety of methods have revealed insights into the chemical bases for these phenomena.

13. Specificity and Stability of Leucine Zipper Interactions. *Peter S. Kim.* Howard Hughes Medical Institute, Whitehead Institute for Biomedical Research, Department of Biology, Massachusetts Institute of Technology, Cambridge, MA 02142.

The leucine zipper motif was originally proposed by McKnight's group as a hypothetical dimerization motif in a new class of DNA binding proteins [Landschulz et al. (1988) *Science 240*, 1759]. Biochemical, spectroscopic, and X-ray crystallographic studies have shown that a synthetic peptide corresponding to the leucine zipper of the yeast transcriptional activator, GCN4, folds as a two-stranded, parallel-coiled coil [O'Shea et al. (1989) *Science 243*, 538; Oas et al. (1990) *Biochemistry 29*, 2891; O'Shea et al. (1991) *Science 254*, 539]. The isolated leucine zipper regions from the nuclear oncogene products, Fos and Jun, are sufficient to mediate specific heterodimer formation [O'Shea et al. (1989) *Science 245*, 646]. This provides a simple model system for studying the specificity of protein–protein interactions: two α-helices that prefer to interact with each other rather than with themselves. It is found that destabilization of the Fos homodimer by acidic residues provides a thermodynamic driving force favoring heterodimers, and that eight amino acid residues from Fos and from Jun are sufficient to direct preferential heterodimer formation [O'Shea et al. (1992) *Cell*, in press].

14. De Novo Design of Helical Proteins. *William F. DeGrado.* Du Pont Merck Pharmaceutical Company, Experimental Station, P.O. Box 80328, Wilmington, DE 19880-0328.

Our group has recently adopted a synthetic approach to understanding the structural basis for protein function. In order to test some of the rules and concepts which are believed to be important for protein folding and stability, we are attempting to design some simple proteins which should fold into predetermined three-dimensional structures. Several types of helical proteins have been designed. The first is a two-stranded coiled coil, a fold found in transcriptional activators and fibrous proteins. Synthetic variants of this motif have been useful for understanding protein folding and DNA recognition. A second protein is an idealized version of a four-helix bundle, a folding pattern found in the structures of a variety of natural water-soluble proteins including myohemerythrin, cytochrome *c'*, and apoferritin. Our initial design folded into a very stable structure, and subsequent designs have added the function of binding specifically to metal ions. A third class of designed proteins is meant to mimic the structures of proteins which form ion channels such as the acetylcholine receptor.

15. Studies of the Mechanism of Ketosteroid Isomerase (KSI) and Its Mutants. *A. S. Mildvan,* A. Kuliopulos, L. Xue, D. Shortle, and P. Talalay. Johns Hopkins School of Medicine, Baltimore, MD 21205.

KSI catalyzes the conversion of Δ^5- to Δ^4-3-ketosteroids by a conservative tautomeric transfer of the 4β-proton to the 6β-position. NMR docking of a spin-labeled substrate analogue into the 2.5-Å X-ray structure of KSI and site-specific mutagenesis identified Tyr-14 and Asp-38 as the general acid and base catalysts. The Y14F and D38N mutants showed $10^{4.7}$- and $10^{5.6}$-fold decreases in k_{cat}, respectively, which were additive in the double mutant, suggesting concerted general acid–base catalysis. Primary and secondary substrate and solvent deuterium kinetic isotope effects with wild-type KSI showed the rate-limiting step to be the concerted enolization of the bound substrate and revealed a tunneling contribution to substrate deprotonation. Consistent with a concerted enolization, NOESY studies of the active double mutant Y55F + Y88F, in which Tyr-14 was the only Tyr residue, revealed an orthogonal arrangement of Asp-38 and Tyr-14 near the enzyme-bound substrate. In contrast to the wild-type enzyme, the D38N mutant shows no stereoselectivity for the 4β-proton and a stepwise enolization with an oxycarbonium ion intermediate. The Y14F mutant shows a stepwise enolization with a carbanion intermediate which dissociates from the enzyme and spontaneously forms substrate and product in solution.

16. Converting Trypsin to Chymotrypsin. *L. Hedstrom,* L. Szilagyi,[1] and W. J. Rutter. Hormone Research Institute, Department of Biochemistry and Biophysics, University of California, San Francisco, CA 94143, and [1]Biochemistry Department, L. Eotvos University, Budapest, Hungary.

The serine proteases trypsin and chymotrypsin have similar tertiary structures, yet display very different substrate specificities: trypsin cleaves peptides at Arg and Lys residues while chymotrypsin prefers large hydrophobic residues. Replacement of the S1 binding site of trypsin with the analogous

residues of chymotrypsin is not sufficient to transfer specificity for amide hydrolysis. Trypsin is converted to a chymotrypsin-like protease when the binding pocket alterations are further modified by exchanging the chymotrypsin surface loops 185–188 and 221–225 for the analogous trypsin loops. These loops are not structural components of either the S1 binding site or the extended substrate binding sites. This mutant enzyme (Tr → Ch[S1 + L1 + L2]) is equivalent to chymotrypsin in k_{cat} and utilizes extended substrate binding to accelerate catalysis like chymotrypsin, though substrate binding is impaired. (The work was supported by NIH DK21344 and is part of an ongoing collaborative project with the laboratory of Laszlo Graf at L. Eotvos University, Budapest.)

17. Subtiligase: An Enzyme Designed for Semisynthesis of Proteins. *James A. Wells*, Thomas Chang, and Lars Abrahmsen. Department of Protein Engineering, Genentech, Inc., South San Francisco, CA 94080.

We have designed variants of the bacterial serine protease, subtilisin, that can effectively ligate peptide bonds in aqueous solution. Subtilisin rapidly hydrolyzes peptides and esters via a reaction mechanism involving formation of an acyl–enzyme intermediate. Kaiser and co-workers [Nakatsuka et al. (1987) *J. Am. Chem. Soc. 109*, 3808–3810] showed that S221C subtilisin, in which the catalytic serine was converted to cysteine, could be used for ligation of peptide bonds because the thiol–acyl intermediate is much more prone to aminolyze than hydrolyze. However, the enzyme was so inactive that highly activated alkyl-ester substrates were required to achieve even slow rates of ligation. By engineering the active site of the enzyme we have produced a double mutant (S221C/P225A) that partially relieves the steric problems created by replacing Ser221 with the larger Cys residue [Abrahmsen et al. (1991) *Biochemistry 30*, 4151–4159]. Finally, we have produced specificity variants of S221C/P225A that allow a variety of sequence junctions to be ligated. Data will be presented that these enzymes can efficiently ligate synthetic peptides into proteins, to be used for incorporating nonnatural amino acids and other structural and functional probes.

18. Investigation of Trypsin D189G/G226D, an Analogue of Human Neutrophil Elastase? *C. Tsu*, J. Perona, M. McGrath, R. Fletterick, and C. Craik. Departments of Pharmaceutical Chemistry and Biochemistry and Biophysics, University of California, San Francisco, CA 94143.

The serine protease trypsin cleaves peptide bonds carboxy terminal to arginine and lysine residues. Aspartic acid 189 is thought to be the determinant of this specificity, forming electrostatic interactions with these positively charged side chains at the base of the primary substrate binding pocket. Glycine 226, located on the opposite wall, allows entrance of the bulky residues into the cavity. Human neutrophil elastase possesses an unusual geometry switch of glycine 189, aspartic acid 226. D189G/G226D rat anionic trypsin has been kinetically and crystallographically characterized. Trypsin D189G/G226D retains up to 16% of wild-type k_{cat} on activated amide substrates. The X-ray crystal structures of trypsin D189G/G226D in complex with BPTI, APPI, and benzamidine have been solved and refined. These results indicate that human neutrophil elastase may have evolved from an alternative trypsin. Valine 216, a glycine in trypsin, could be responsible for blocking this specificity in the present enzyme.

19. Aspartate-99 of the Phospholipase A2 Catalytic Diad Has both Catalytic and Structural Roles. *C. M. Dupureur*, B.-Z. Yu, Y. Li, M. Jain, and M.-D. Tsai. Department of Chemistry, Ohio State University, Columbus, OH 43210, and Department of Chemistry, University of Delaware, Wilmington, DE 19716.

Histidine-48 and aspartate-99 form the absolutely conserved "catalytic diad" in phospholipase A2. To better understand the reaction mechanism, we have examined structure–function relationships for Asp-99 and found it to have critical roles in both catalysis and conformation. The mutant enzyme D99N (aspartate to asparagine) has significantly decreased activity relative to wild type. Examination of the details of binding and catalysis indicates that the chemical step is rate-limiting, suggesting a catalytic role for Asp-99. Interestingly, the conformational stability of D99N is half that of wild-type. Structural evaluation of the mutant enzyme by NMR confirms that this enzyme is conformationally distinct from wild type and suggests that Asp-99 may have important structural roles as well.

20. A 70-Kilodalton Heat Shock Cognate Protein: Surprises in a Partial Structure. *D. B. McKay*. Department of Cell Biology, Stanford University Medical Center, Stanford, CA 94305.

A major focus of our studies on molecular chaperones has been the constitutively expressed bovine 70-kDa heat shock cognate protein (HSC70). We have isolated, crystallized, and solved the structure of a 44-kDa amino-terminal ATPase fragment of HSC70, and have found that it has a two-lobe, four-domain structure, with the nucleotide bound at the base of a cleft between the lobes. Surprisingly, despite the lack of global sequence similarity between the HSP70-related proteins and other protein families, the tertiary fold of the nucleotide binding portion of the structure is similar to that of hexokinase, and the fold of the entire molecule closely resembles that of actin; this similarity suggests mechanistic experiments which are currently being pursued.

21. Crystallographic Analysis of Steroid Receptor–DNA Interactions. WeiXin Xu, Ben Luisi, Zbyszek Otwinowski, Len Freedman,[1] Keith Yamamoto,[1] and *Paul B. Sigler*. Department of Molecular Biophysics and Biology and Howard Hughes Medical Institute, Yale University, New Haven, CT 06511, and [1]Department of Biochemistry and Biophysics, University of California, San Francisco, CA.

We have determined the crystal structure of two complexes formed by the glucocorticoid receptor's DNA-binding domain and DNA. The domain has a globular fold which contains two Zn-nucleated substructures of distinct conformation and function. When it binds DNA, the domain dimerizes, placing the subunits in adjacent major grooves of the target. The principal structure is refined to 2.5 Å and contains a modified target in which the spacing between the half-sites is enlarged by one base pair. This results in one subunit interacting specifically with the consensus target half-site and the other nonspecifically with a noncognate element. A second structure is refined to 3.5 Å and shows specific and symmetrical to both half-sites of a target containing the canonical three-base pair spacing. We identify the interactions responsible for 'recognition' of the half-site. The novel feature of this complex is that a very strong dimer interface is produced when the subunits interact with DNA. This DNA-induced dimer fixes the separation of the subunits' recognition surfaces so that the spacing between the half-sites becomes a critical feature of the target sequence's identity.

22. Complex between Growth Hormone and the Extracellular Domain of Its Receptor. *A. M. de Vos*, M. Ultsch, and A. A. Kossiakoff. Department of Protein Engineering, Genentech, Inc., South San Francisco, CA 94080.

Binding of human growth hormone to its receptor is one of the steps required for the regulation of normal human growth and development. The 2.8-Å crystal structure of the complex between the hormone (hGH) and the extracellular domain of its receptor (hGHbp) shows the complex to consist of one growth hormone and two receptor molecules. hGH is a four-helix bundle having an unusual topology. The hGHbp consists of two distinct domains, similar in some respects to immunoglobulin domains. These domains, however, have a relative orientation very different from that found between constant and variable domains in immunoglobulin Fab fragments. Both hGHbp domains contribute residues involved in hGH binding. Surprisingly, in the complex both receptors use essentially the same residues even though the two binding sites on hGH have no structural similarity. Generally, the hormone–receptor interfaces match those identified by previous mutational analyses. In addition to the hormone–receptor interfaces, there is also a substantial contact surface between the C-terminal domains of the receptors. The relative extents of the contact areas support a sequential mechanism for dimerization.

23. Structural Changes in a Transmembrane Receptor: Crystal Structures of the Ligand Domain of Aspartate Chemotaxis Receptor with and without Aspartate. Michael V. Milburn,[1] Gilbert G. Prive,[1] William G. Scott,[1] Daniel L. Milligan,[2] Joanne Yeh,[1] Jarmilla Jancarik,[1] Daniel E. Koshland, Jr.,[2] and *Sung-Hou Kim.*[1] [1]Department of Chemistry and Lawrence Berkeley Laboratory, and [2]Department of Molecular and Cell Biology, University of California, Berkeley, CA 94720.

Most transmembrane receptors receive information by binding specific ligands in the ligand domains and transmit the information through the transmembrane domains to the cytoplasmic effector domains. The detailed mechanism of the signal transmission is not known. In this report we present and compare the X-ray crystal structures of the apo and the complex between aspartate and the ligand domain dimer of a bacterial transmembrane receptor. The structure reveals that the aspartate binds at the subunit interface between two α-helices from one monomer and another α-helix from the other monomer. The aspartate binding does not change the conformation of monomers significantly but alters the relative orientation of one monomer with respect to the other and locks together the two monomers, stabilizing the activated form. Implications of the structural changes on signal transduction will be discussed.

24. Perhydroxyl Radical (HOO•) and Lipid Hydroperoxide Initiated Lipid Peroxidation in Large Unilamellar Liposomes. *John Aikens*[1] and Thomas A. Dix.[1,2] Departments of [1]Chemistry and [2]Biological Chemistry, The University of California, Irvine, CA 92717.

Initiation of lipid peroxidation by the perhydroxyl radical (HOO•) source xanthine oxidase was studied in large unilamellar liposome vesicles (LUVs) prepared from dilinoleoylphosphatidylcholine (di-18:2-PC). In agreement with previous studies performed in fatty acid dispersions [Aikens, J., & Dix, T. A. (1991) *J. Biol. Chem. 266*, 15091], HOO• initiated lipid peroxidation only if hydroperoxides (LOOHs, either fatty acid- or di-18:2-PC-derived) were included in the LUVs. Alterations in observed rates of oxidation between lipid dispersions and LUVs resulted from differences in substrate environment. Lipid product studies were consistent with the earlier hypothesis of a hydrogen atom transfer mechanism between HOO• and LOOH to form peroxyl radicals, the chain propagating species of lipid peroxidation. Fluorescence leakage experiments and gross structural analysis of LUVs by laser light scattering provided evidence that the addition of LOOHs alters the permeability of the membrane without affecting liposome size, which may increase the lipid's accessibility to exogeneously formed oxidants. Lipid peroxidation is implicated in many pathological processes; this study supports an alternative mechanistic hypothesis for lipid peroxidation initiation that may be operative in vivo.

25. Novel, Viable Mechanisms for Dioxygen Activation in Monooxygenases Revealed by Recent Site-Directed Mutagenesis Studies of Cytochrome P450cam. *P. Chandrasekhar* and G. V. Kulkarni. Gumbs Associates, Inc., 11 Harts Lane, East Brunswick, NJ 08816.

Recent key studies on site-directed mutagenesis of cytochrome P450cam have revealed that substitution of the Thr-252 residue adjacent to the active site by nonhydrophilic alanine or valine drastically uncouples the monooxygenase pathway, whereas OH-containing residues such as serine retain monooxygenase activity. We use semiempirical quantum chemical studies to propose a novel mechanism for O_2 activation that accounts for these effects. Based on earlier work where metal $d_\pi \rightarrow \sigma^*$ back-donation was shown to lead to facile O–O bond cleavage, the results reveal that back-donation from water lone pairs into the coordinated O_2 σ^* orbitals can lead to facile O–O cleavage, with split distal O absorbed by substrate. An analysis of the energetics of this normally unlikely interaction and comparison with free O_2 and free peroxo cases reveals that metal coordination of O_2 drastically lowers the repulsive energy barrier for the interaction. In addition to metal, presence of substrate to accept the split O is necessary in this activation mode. Thr-252 in P450cam functions to retain water molecules (via H-bonding) for this. The metalloxo-Fe(IV)=O species is shown to be a product, not a reactant, in oxygenation.

26. Transition Metal Ion Activation of Dioxygen in Monooxygenases: Novel, Viable Mechanisms with Water as Unexpected Key Player in Activation. *P. Chandrasekhar* and G. V. Kulkarni. Gumbs Associates, Inc., 11 Harts Lane, East Brunswick, NJ 08816.

A novel mechanism for dioxygen activation in monooxygenases is presented involving a crucial role for water. The work uses as a basis the large body of available experimental data and earlier work in which transition metal $d_\pi \rightarrow O_2$ σ^* back-donation was shown to lead to facile O–O bond cleavage, and it employs semiempirical quantum chemical methods. The most relevant results from more than 1500 calculations on distinct geometries are reported. It is shown that back-donation from water lone pairs into a coordinated O_2 σ^* orbital leads to facile O–O cleavage. An analysis of the energetics of this normally unlikely interaction and comparison with free O_2 and free peroxo cases reveals that metal coordination of O_2 drastically lowers the repulsive energy barrier for the interaction. In addition to metal coordination of O_2, the presence of substrate capable of accepting the split distal O is necessary for this activation mode. Application to the crystal structure of cytochrome P450cam is then demonstrated. Here the mechanism accounts for the effect of Thr-252 substitution and the presence of the water molecule cluster. The metalloxo-

Fe(IV)=O species is shown to be a product, not a reactant, in oxygenation.

27. Elimination Reactions Catalyzed by Soybean Lipoxygenase. *C. H. Clapp*, A. M. Grandizio, J. M. Aurand, and R. Moser. Department of Chemistry, Bucknell University, Lewisburg, PA 17837.

The ferric form of soybean lipoxygenase catalyzes an elimination reaction on 12-iodo-*cis*-9-octadecenoic acid to produce iodide ions and 9,11-octadecadienoic acid (9,11-ODA). This reaction is accompanied by irreversible inactivation of the enzyme on about one out of eight turnovers. Neither elimination nor inactivation is observed with the ferrous form of the enzyme. Free-radical scavengers protect the enzyme from inactivation but do not inhibit the elimination reaction. Ferric lipoxygenase also catalyzes the conversion of 12-bromo-*cis*-9-octadecenoic acid to 9,11-ODA, but in this case the enzyme is not inactivated. Possible mechanisms for these reactions and their implications for the normal catalytic mechanism of lipoxygenase will be discussed.

28. Reduction of Cytochrome *c* Peroxidase Compounds I and II by Ferrocytochrome *c*: pH Dependence. *Malcolm J. D'Souza* and James E. Erman. Department of Chemistry, Northern Illinois University, DeKalb, IL 60115.

The reduction of cytochrome *c* peroxidase compound I by excess ferrocytochrome *c* has been investigated by stopped-flow techniques between pH 4 and 8 at 10 mM ionic strength. Reduction of compound I is consistent with a mechanism involving complex formation between the two proteins, followed by intracomplex electron transfer, reducing the Fe(IV) site in compound I. The apparent bimolecular rate constant for the interaction between compound I and cytochrome *c* is relatively independent of pH between pH 5.5 and 8.0 in phosphate buffers. Reduction of compound II by ferrocytochrome *c* is anomalous. The rate of reduction is independent of the cytochrome *c* concentration and is second-order with respect to the peroxidase. The latter observation suggests that a rate-limiting bimolecular reaction between peroxidase species is required for reduction of compound II under the conditions of our experiments. The apparent bimolecular rate constant for this rate-limiting step is independent of pH between pH 4 and 8 with a value of $5.1 \pm 1.5 \times 10^7$ M^{-1} s^{-1}.

29. Homology Modeling of Lignin Peroxidase. *Ping Du*, Jack R. Collins, and Gilda H. Loew. Molecular Research Institute, 845 Page Mill Road, Palo Alto, CA 94304.

A three-dimensional model of lignin peroxidase (LiP) has been constructed based on sequence alignments and the crystal structure of cytochrome *c* peroxidase (CCP). Model constructions were carried out with successive constrained energy minimization and molecular dynamics (MD) simulations. Results from fully solvated protein MD simulations were used to identify the conformationally unstable regions of the model. The predicted structure reveals three major aspects: (A) Four disulfide bonds were predicted; (B) The model suggests that Arg48 is not the origin of the observed pH dependence of LiP activity near pH 1; (C) Two substrate binding site candidates with flexible surface aromatic residues were located. These properties are consistent with the fact that LiP binds a variety of aromatic substrates of different sizes, ranging from lignin, methoxybenzenes, to polycyclic aromatic hydrocarbons.

30. Timing a Cytochrome P-450 Reaction: Epoxidation of a Radical Clock Olefin. *Julia A. Fruetel*, Vaughn P. Miller, and Paul R. Ortiz de Montellano. Department of Pharmaceutical Chemistry, S-926, University of California, San Francisco, CA 94143.

The mechanism for olefin epoxidation by cytochromes P-450 is not well established, although model heme studies have suggested the possible intermediacy of radical, cationic, or radical–cationic intermediates. To test whether or not such intermediates are involved in the enzyme reaction, the metabolites from incubation of the radical clock olefin *trans*-2-phenyl-1-vinylcyclopropane with cytochrome $P450_{cam}$ were analyzed. No cyclopropane ring-opened metabolites other than those derived from the epoxide are observed. Lack of detection of any cytochrome $P450_{cam}$-dependent ring-opened products indicates that the epoxidation reaction proceeds at a rate greater than that of the ring-opening—i.e., on the order of 10^{12} s^{-1}. The speed of this reaction makes the intermediacy of neutral radical species unlikely.

31. High-Performance Liquid Chromatographic Analysis of Lipid Peroxides in Fish Oil. J. I. Teng[1] and *N. M. Made Gowda*.[2] [1]Department of Human Biological Chemistry and Genetics, University of Texas Medical Branch, Galveston, TX 77550, and [2]Department of Chemistry, Western Illinois University, Macomb, IL 61455.

Menhaden fish oil containing fatty acid esters was subjected to alkaline hydrolysis in the presence of air at room temperature for 24 h. The hydrolysate was acidified, and the fatty acids were extracted with hexane. The fatty acids were then separated by TLC, using a solvent system of hexane–acetic acid–water (100:5:2.5), into three groups: (a) a combination of saturated and monounsaturated fatty acids; (b) a mixture of polyunsaturated fatty acids (PUFAs); and (c) a mixture of peroxide-positive fatty acids as determined by Wurster dye test. Analysis of group b material on a Waters Associates HPLC instrument using fatty acid columns with a mobile phase of THF–acetonitrile–water–acetic acid (25:35:75:0.4) gave four major peaks corresponding to the PUFAs, 18:3n-3, 20:5n-3, 20:4n-6, and 22:6n-3. The chromatogram of group c material obtained with the same column and solvent system showed five distinct peaks for peroxides. The characterization of these fatty acid hydroperoxides is currently under investigation. (This work has been supported by Grant N-06 from the American Heart Association—Illinois Affiliate.)

32. Oxygenation versus Electron Abstraction by HRP Is Determined by the Location of Substrate Binding. *Robert Z. Harris* and Paul R. Ortiz de Montellano. Department of Pharmaceutical Chemistry, University of California, San Francisco, CA 94143-0446.

Horseradish peroxidase (HRP) enantioselectively oxidizes thioanisole to the (*S*)-(−)-sulfoxide in 70% enantiomeric excess. The sulfide oxygen is derived primarily from hydrogen peroxide. Para substitution of thioanisole with electron-donating or -withdrawing groups does not significantly alter the enantioselectivity. HRP reconstituted with δ-*meso*-ethylheme or preincubated with phenylhydrazine is not able to oxidize guaiacol yet is fully able to oxidize thioanisole. The enantiomeric excess of the product sulfoxide is 26% and 28% for the δ-*meso*-ethylheme-reconstituted and phenylhydrazine-treated species, respectively. Thioanisole noncompetitively inhibits guaiacol oxidation by HRP. These results suggest that the thioanisole binding site is distinct from the guaiacol binding site, and that the binding site may dictate whether HRP exhibits oxidase or peroxidase activity. (Supported by NIH Grant GM 32488.)

33. Evaluation and Application of *N*-Hydroxy-2-thiopyridone as a Nonmetal-Dependent Source of the Hydroxyl Radical in Aqueous Systems. *Kathleen M. Hess*[1] and Thomas A. Dix.[1,2] Departments of [1]Chemistry and [2]Biological Chemistry, University of California, Irvine, CA 92717.

N-Hydroxy-2-thiopyridone (**1**), an established source of the hydroxyl radical [HO•; Boivin, J., Crepon, E., & Zard, S. Z. (1991) *Tetrahedron Lett. 31*, 6869], was demonstrated to produce HO• under conditions directly amenable to biological studies. Generation of HO• was monitored in the following 'HO•' assays: deoxyribose degradation, addition to DMSO, and hydroxylation of salicylate and phenol. All four assays demonstrated the production of HO• from **1** (added as its sodium salt) under mild conditions in aqueous buffer systems; an improved analysis method was developed for the phenol assay. A time course analysis demonstrated that a flux of HO• is generated from **1** throughout the irradiation period. Direct application of **1** as a HO• generator was demonstrated in in vitro studies of lipid peroxidation which identified specific HO•-associated oxidation products.

34. Subunit Isolation for Active Site Identification of *Methylosinus trichosporium* OB3b Soluble Methane Monooxygenase. *M. M. Himmelsbach*, R. T. Taylor, and M. W. Droege. Lawrence Livermore National Laboratory, Livermore, CA 94550.

Understanding the complex catalytic behavior of the cytosolic methane monooxygenase (sMMO) enzyme system will require a more thorough knowledge of the active pocket where methane functionalization occurs. This soluble enzyme system is known to be composed of three proteins: A, B, and C. Substrate oxidation is believed to occur at a binuclear iron center in protein A. It has a molecular weight of 245 000 Da and is an oligomeric protein with three distinct subunits in an $\alpha_2\beta_2\gamma_2$ configuration. Of particular interest to us are the chemical identities of amino acids surrounding the active site iron atoms. In order to stockpile milligram quantities of each subunit and later to simplify the purification of active site polypeptide fragments, we have devised a scheme for the resolution and separation of the α, β, and γ subunits from purified sMMO protein A, which was derived from a methanotrophic bacterium, *M. trichosporium* OB3b. Conditions were first developed for the dissociation of the three distinct polypeptide subunits. The isolation of these subunits, under denaturing conditions, was then achieved by utilizing the net charge differences between the subunits to effect a separation by anion-exchange chromatography. (Work performed under the auspices of the Department of Energy by LLNL, Contract W-7405-ENG-48.)

35. Magnetic Field Effect Studies of Lipoxygenase-Catalyzed Oxidation of Linoleic Acid. *Chi-Ching Hwang* and Charles B. Grissom. Department of Chemistry, University of Utah, Salt Lake City, UT 84112.

The effect of a static magnetic field on the rate of soybean lipoxygenase catalyzed oxygenation of linoleic acid was determined. The kinetic parameters V_{max}, K_m, and V_{max}/K_m are unaffected by magnetic fields 0–2000 G. This result is unexpected in light of the proposed radical mechanism of soybean lipoxygenase. As a further probe of the reaction mechanism, the effect of a static magnetic field on the deuterium and tritium kinetic isotope effect has been determined. This allows discrimination between possible magnetic isotope effect interactions and hydrogen tunneling contributions to the observed kinetic isotope effect.

36. Catalysis of Sulfite Oxidation by Aquocobalamin and Cyanoaquocobinamide. *J. Ji* and D. W. Jacobsen. Department of Chemistry, Cleveland State University, Cleveland, OH 44115, and Departments of Brain and Vascular Research and Laboratory Hematology, Research Institute, Cleveland Clinic Foundation, Cleveland, OH 44195.

Cobalamins (Cbl, B12) and cobinamides (Cbi) catalyze the oxidation of mono- and dithiols in the presence of O_2 to disulfides and cyclic disulfides, respectively [Jacobsen et al. (1989) *Biochemistry 23*, 2017]. Pseudo-first-order rate constants (k_1) for the catalysis of 2-mercaptoethanol oxidation at pH 8.5 by aquocobalamin (aqCbl) and cyanoaquocobinamide (CN-Cbi) were 0.18 and 191 s^{-1}, respectively. In this study we describe the ability of aqCbl and CN-Cbi to catalyze the oxidation of sodium sulfite and describe some of the properties of the reaction including product identification. Pseudo-first-order rate constants were determined by following the disappearance of O_2 with a Clark electrode. The catalysis of sulfite oxidation by aqCbl and CN-Cbi was both pH and light dependent. At pH 6.00 under tungsten-filament illumination, $k_1 = 1.71$ s^{-1} for aqCbl-catalyzed sulfite oxidation. The dark reaction was zero under similar conditions. At pH 7.00 under tungsten-filament illumination, $k_1 = 0.30$ s^{-1} for CN-Cbi-catalyzed sulfite oxidation. The dark reaction was zero. The product of the aqCbl- and CN-Cbi-catalyzed reactions was identified as SO_4^{2-} by capillary electrophoresis with indirect spectrophotometric detection. The ability of corrinoids to catalyze sulfite oxidation may explain the efficacy of these compounds in blocking sulfite-induced hypersensitivity reactions in chronic asthmatic patients.

37. Free Chlorine Species Are Not Involved in Chloroperoxidase Catalyzed Chlorination Reactions of Good Substrates. *R. Daniel Libby*, Tina M. Beachy, and A. Kathryn Phipps. Department of Chemistry, Colby College, Waterville, ME 04901.

Chloroperoxidase occupies a key position among hemoproteins. It catalyzes the reactions characteristic of peroxidases, catalase, and some cytochrome P_{450} monooxygenases. Halide ions are substrates for peroxidatic halogenation reactions, and although the peroxidatic and catalatic reactions catalyzed by CPO do not consume halide ions, at least some of them are accelerated by the presence of chloride. Over the last several years, there has been considerable controversy as to the exact mechanism of halogen atom transfer from the enzyme to halogenation substrates. Some reports favor direct transfer of the halogen atom from the enzyme to the substrate, while others argue for the intermediacy of a nonenzymatic halogenating agent. This study used comparisons of substrate specificities as well as inhibition studies to investigate the possibility of the involvement of a freely dissociable oxidized halogen as an intermediate in CPO-catalyzed reactions. Results indicate that a freely dissociable species, probably Cl_2, is involved in reactions of substrates with relatively high K_M values but that the halogen is directly transferred from the enzyme to substrates with low K_M values. This latter class of substrates includes almost all "good" halogenation substrates for CPO.

38. Monooxygenase Activity of Cytochrome *c* Peroxidase. *Vaughn P. Miller*,[1] Gia D. DePillis,[1] Juan C. Ferrer,[2] A. Grant Mauk,[2] and Paul R. Ortiz de Montellano.[1] [1]Department of Pharmaceutical Chemistry, University of California, San

Francisco, CA 94143-0446, and [2]Department of Biochemistry, University of British Columbia, Vancouver, BC, V6T 1Z3 Canada.

Recombinant cytochrome *c* peroxidase (CcP) and a W51A mutant of CcP, in contrast to other classical peroxidases, react with phenylhydrazine to give σ-bonded phenyl–iron complexes, suggesting that the heme iron is accessible to substrates. This conclusion is supported by the observation that CcP and W51A CcP oxidize thioanisole to the racemic sulfoxide with quantitative incorporation of oxygen from H_2O_2. Definitive evidence for an open active site is provided by stereoselective epoxidation of styrene, *cis*-β-methylstyrene, and *trans*-β-methylstyrene by both enzymes. These epoxides are likewise formed via ferryl oxygen transfer mechanisms because their oxygen also derives from H_2O_2. The phenyl–iron complex is not formed, and substrate oxidation is not observed when the prosthetic group is replaced by δ-*meso*-ethylheme. Our results indicate that the ferryl (Fe^{IV}=O)/protein radical pair found in CcP can be coupled to achieve two-electron oxidations. The unique ability of CcP to catalyze monooxygenation reactions does not conflict with its peroxidase function since cytochrome *c* is oxidized at a distant surface location [Depillis, G. D., Sishta, B. P., Mauk, A. G., & Ortiz de Montellano, P. R. (1991) *J. Biol. Chem. 266*, 19334–19341]. (This work was supported by National Institutes of Health Grant GM32488.)

39. The Mechanism of Fatty Acid Oxygenation by Lipoxygenase. *Mark J. Nelson* and Rebecca A. Cowling. Du Pont, Wilmington, DE 19880-0328. Steven P. Seitz. Du Pont Merck Pharmaceuticals, Wilmington, DE 19880-0353. Robert C. Scarrow and Geoffrey Grove. Haverford College, Haverford, PA 19041.

We have studied the active ferric and purple forms of soybean lipoxygenase by EPR and EXAFS spectroscopies. The iron is coordinated by nitrogen and/or oxygen donor ligands, probably including one hydroxide. The apparent high-reduction potential of the iron is consistent with the remainder of the ligands being primarily neutral, e.g., imidazole. We see production of two radical species upon treatment of ferric lipoxygenase with either substrates or products to form "purple" lipoxygenase. One is probably a fatty acid peroxyl radical. The other is a fatty acid alkyl radical whose structure we are determining by assigning the hyperfine couplings observed in the EPR spectrum via deuterium labeling. The line shapes and saturation behavior of these radicals are consistent with their being bound to the enzyme in proximity to the iron. The possible relevance of these radicals to the oxygenation and peroxidase reactions catalyzed by lipoxygenase is being explored.

40. Iodide Oxidation by Horseradish Peroxidase: Characterization of the Iodide Binding Site. *Sherri L. Newmyer* and Paul R. Ortiz de Montellano. Department of Pharmaceutical Chemistry, University of California, San Francisco, CA 94143-0446.

Iodide oxidation, catalyzed by horseradish peroxidase (HRP), was investigated to differentiate binding of iodide relative to that of guaiacol, a classic HRP substrate. Reconstituting HRP with δ-mesoethylheme blocked enzymatic oxidation of both substrates. Reconstitution with δ-mesomethylheme gave native-like iodide activity and slightly increased guaiacol activity. Arylating HRP with phenylhydrazine essentially destroyed both activities. Inhibition studies showed that guaiacol and thioanisole, another nonclassic HRP oxidant, altered iodide activity. These studies suggest that iodide has a binding site that overlaps the guaiacol and thioanisole sites, yet is distinct. This binding mode could be used to explain the observed atypical electron abstraction seen with iodide oxidation. (This work was supported by Grant GM32488.)

41. pH-Dependence of NAD^+ Solvolysis in 1:1 Water–Methanol Mixtures. *Norman J. Oppenheimer* and Rachel Tashma. Department of Pharmaceutical Chemistry, University of California San Francisco, San Francisco, CA 94143.

The pH-dependence of the stereospecificity and stereoselectivity of the solvolysis of NAD^+ in 1:1 water–methanol mixtures has been measured by HPLC, and the products were confirmed by ^1H NMR and LSIMS mass spectrometry. The stereospecificity of methanolysis is strongly dependent on the pH. Inversion is favored by 22 ± 2:1 for the pH-independent reaction below pH 6.5 while retention is favored by 24 ± 3:1 for the pH-independent reaction above pH 12.5. In contrast, over the pH range 4.5–13.6 the ratio of hydrolysis to methanolysis (selectivity) remains ca. 1. The implication of these results for the mechanism of hydrolysis of NAD^+ will be discussed. (Supported in part by NIH Grant GM-22982.)

42. The Question of the Mechanism of Proton Pumping in Cytochrome *c* Oxidase. *Jim Peterson* and David E. Holm. Department of Chemistry, The University of Alabama, Tuscaloosa, AL 35487-0336. Gerald Godette, Celia Bonaventura, and Joseph Bonaventura. Duke University Marine Biomedical Center, Beaufort, NC 28516.

Theories of how proton translocation across the mitochondrial membrane is coupled to electron transfer in cytochrome *c* oxidase fall into two broad categories; namely, those that do and those that do not involve direct coupling at the metal centers. Magnetic circular dichroism (MCD) spectroscopy is especially suitable for investigating the latter type of mechanism, since signals attributable to three of the four metal centers may be observed in the near-infrared region of the spectrum, essentially free of overlap. We have begun a study of various *pulsed* cytochrome *c* oxidase derivatives on the enzyme isolated from beef and shark sources by low-temperature MCD spectroscopy. The aim is to search for pH-dependent changes in the spectra, suggesting proton-exchange activity in the coordination shells of the metal centers, thereby indicating potential candidates for the site of coupling of electron transfer to proton translocation. Initial results will be presented and the reasons for wishing to use the shark enzyme discussed.

43. Identification of Heme Axial Ligands in the Cytochrome *d* Complex of *Escherichia coli*. *Jim Peterson*. Department of Chemistry, The University of Alabama, Tuscaloosa, AL 35487-0336. Tamma Zuberi and Robert B. Gennis. Department of Biochemistry and Chemistry, University of Illinois, Urbana, IL 61801.

Near-infrared MCD spectroscopy of low-spin ferric hemes, in conjunction with EPR measurements, is often capable of unambiguously assigning the type of axial ligands present. We have recorded such data for the cytochrome *d* complex (containing heme *d*, heme b_{558}, and heme b_{595}) and for a mutant containing only cytochrome b_{558}. An interesting puzzle has arisen out of this work in that it appears as though the mutant b_{558} may have different axial ligands than the same heme in the wild-type protein. Alternately, all the hemes are in some

way connected in the cytochrome *d* complex, leading to some unusual features in the spectra.

44. Kinetic Characterization of Prokaryotic Urate Oxidase. *Mark T. Smith* and Peter A. Tipton. Department of Biochemistry, University of Missouri, Columbia, MO 65212.

Urate oxidase catalyzes the oxidation of uric acid by oxygen, producing allantoin, H_2O_2, and CO_2. We have isolated urate oxidase from *Bacillus fastidiousus* and initiated steady-state kinetic studies. Initial velocity studies in air-saturated buffer yielded a K_m for urate of 140 μM. Although earlier studies of the enzyme from pig liver suggested that urate oxidase catalyzes the formation of an unstable species which decays nonenzymatically to allantoin, we see no evidence for the formation of this species. Allantoin showed no inhibition versus urate at concentrations up to 1 mM. Oxonate, a potent inhibitor (K_i = 2 μM), showed a noncompetitive inhibition pattern versus urate, in contrast to the competitive inhibition seen with the pig liver enzyme. Further kinetic studies are in progress to elucidate the enzyme mechanism.

45. Kinetic Characterization of the Catalytic Activities of Tartrate Dehydrogenase. *Peter A. Tipton* and Ronald L. Koder. Department of Biochemistry, University of Missouri, Columbia, MO 65212.

Tartrate dehydrogenase catalyzes the NAD^+-dependent oxidation of (+)-tartrate, the oxidative decarboxylation of D-malate, and the net nonoxidative decarboxylation of *meso*-tartrate, in the presence of Mn^{2+} and a monovalent cation. We have undertaken a detailed steady-state kinetic analysis of these reactions in order to characterize the enzyme–substrate interactions which determine the course of each catalytic reaction. Kinetic isotope effect studies indicate that hydride transfer from either (+)-tartrate or D-malate to NAD^+ is only partially rate-limiting; comparison of $^D(V/K)$ and $^T(V/K)$ in the D-malate reaction leads to a calculated value of 3.9 for ^Dk. $^T(V/K)_{D\text{-malate}}$ decreases with increasing solution viscosity; the data were fitted to a simple model which allowed us to calculate values of 2.3 for both the internal and external portions of the forward commitment. We are also exploring the specificity of the enzyme for NAD^+ analogues in order to determine whether we can manipulate the outcome of the catalytic reactions by changing the pyridine nucleotide cofactor.

46. The Role of Tyrosine Residues in the Peroxide-Dependent Reactions of Myoglobin. *Angela Wilks*, Satish I. Rao, and Paul R. Ortiz de Montellano. Department of Pharmaceutical Chemistry, University of California, San Francisco, CA 94143-0446.

A synthetic gene-encoding sperm whale myoglobin has been constructed and expressed in *E. coli* DH5α. Site-specific mutagenesis has been used to prepare the single tyrosine to phenylalanine mutants (Tyr-103, -146, and -151) as well as the double and triple constructs. EPR and absorption spectroscopy studies show the wild-type and mutant proteins react with H_2O_2 to give a ferryl species and a protein radical. Cross-linking studies show the radical to be delocalized to Tyr-151, which is required for dimerization of the protein. Incorporation of oxygen from both molecular O_2 and H_2O_2 in the epoxidation of styrene indicates that two mechanisms are involved in this reaction. The incorporation of molecular O_2 is postulated to come from a peroxy radical formed from the addition of O_2 to the protein radical. Studies on oxygen incorporation with both the wild-type and mutant proteins indicate that the tyrosine residues are not absolutely required for this reaction.

47. Purification and Characterization of a Truncated Form of Mammalian Squalene Synthetase. *B. R. Boettcher*,[1] I. Shechter,[2] E. Klinger,[3] M. L. Rucker,[1] R. G. Engstrom,[1] J. A. Spirito,[1] M. A. Islam,[1] S. Cornell,[1] and D. B. Weinstein.[1] [1]Sandoz Research Institute, East Hanover, NJ 07936, [2]Eleanor Roosevelt Institute, Denver, CO 80206, and [3]Tel Aviv University, Tel Aviv, Israel.

Squalene synthetase is a membrane-associated enzyme involved in cholesterol biosynthesis in mammalian systems. The enzyme catalyzes the condensation of two molecules of farnesyl pyrophosphate to form the cyclopropyl ring containing intermediate presqualene pyrophosphate. The enzyme further catalyzes the rearrangement and reduction with NADPH of presqualene pyrophosphate to form squalene. The present work describes the facile purification of mammalian squalene synthetase from rat liver microsomes. The procedure includes induction of the enzymatic activity by treatment of rats with fluvastatin and cholestyramine. This treatment results in approximately a 15–25-fold enhancement of specific activity. The membrane-bound enzyme was then solubilized by controlled proteolysis with trypsin and purified to homogeneity using standard chromatographic procedures. The purified enzyme was characterized with respect to initial velocity kinetics and physical properties. The molecular mass of the truncated enzyme was estimated to be 35 kDa with Superose 12 gel filtration chromatography and 33 kDa with SDS–PAGE gels. In addition, rabbit polyclonal antibodies were prepared against the enzyme. Western blot analysis of liver microsomes indicated a molecular mass of approximately 45–47 kDa for the intact rat hepatic enzyme.

48. Cloning and Overexpression of 4-Oxalocrotonate Tautomerase, an Enzyme with 62 Amino Acid Residues per Subunit. *Lorenzo H. Chen*,[1] George L. Kenyon,[1] Francois Curtin,[2] Shigeaki Harayama,[2] Michael E. Bombanek,[3] Gholamhossein Hajipour,[3] and Christian P. Whitman.[3] [1]Department of Pharmaceutical Chemistry, University of California, San Francisco, CA 94143, [2]Department of Medical Biochemistry, University of Geneva, Geneva, Switzerland, and [3]Medicinal Chemistry Division, University of Texas, Austin, TX 78712.

The *xyl*H gene encoding 4-oxalocrotonate tautomerase (4-OT) has been isolated from a subclone of the *Pseudomonas putida* TOL plasmid and cloned into an *Escherichia coli* vector such that functional 4-OT is expressed in yields of at least 10 mg of pure enzyme per liter of culture. The functional unit is apparently a pentamer of identical subunits, each consisting of only 62 amino acid residues. The amino acid sequence, determined in part from automated Edman degradation and also deduced from the primary sequence of *xyl*H, showed homology neither with any sequences in the current databases nor with any enzymes that catalyze similar reactions. We propose that the active site may be established by an overlap of subunits and comprised of amino acid residues belonging to several, if not all, of the subunits.

49. Cloning and Sequencing of the Gene Encoding Guanosine Kinase from *E. coli*. *Kenneth W. Harlow*. Institute of Biochemical Genetics B, Øster Farimagsgade 2A, DK-1353, Copenhagen K, Denmark. Bjarne Hove-Jensen. Institute of Biological Chemistry B, Sølvgade 83, DK-1307, Copenhagen K, Denmark.

The gene encoding guanosine kinase activity (*gsk*) from *E. coli* has been cloned from the Kohara library by complementation. *E. coli* strain SØ445 (*purE deoD gsk*) requires a functional enzyme for growth on guanosine as a sole purine source. To our knowledge, this is the first purine ribonucleoside kinase to be cloned. The nucleotide sequence of the gene has been determined, and overexpression, purification, and characterization of the gene product are underway. This purine ribonucleoside kinase is capable of phosphorylating guanosine and inosine to their corresponding 5′-nucleoside monophosphates and may play a role in the reutilization of endogenous purine nucleosides in vivo in *E. coli*. Because of the importance of many purine nucleoside analogues in the therapy of a diverse number of diseases in humans, an understanding of the biochemistry of guanosine kinase may be important in understanding the mode of action and metabolism of these drugs in vivo. We hope to extend the knowledge gained from our study of the bacterial enzyme to eukaryotic, particularly human, systems in the future.

50. Engineering an Improved CO_2/O_2 Specificity for *R. rubrum* Ribulose-bisphosphate (RuBP) Carboxylase/Oxygenase. *Mark R. Harpel* and Fred C. Hartman. Biology Division, Oak Ridge National Laboratory, Oak Ridge, TN 37831.

RuBP carboxylase/oxygenase is bifunctional, facilitating addition of either CO_2 or O_2 to the enediol(ate) of RuBP formed in the first step of catalysis. Although carboxylation efficiency is crucial to photosynthetic growth, the enzymic determinants that discriminate between CO_2 and O_2 are unclear. Site-directed replacement of an active-site Ser (S368A) of the *R. rubrum* enzyme effects an ~50% increase in τ, the ratio of V/K for carboxylation vs oxygenation. This is the first alteration of the carboxylase, outside of natural evolution to the more efficient plant enzymes, which improves τ. S368A catalyzes carboxylation at only 1–2% of the wild-type rate with minimal changes in K_m for RuBP or CO_2. However, the apparent O_2 affinity is drastically reduced; S368A is not inhibited by 1.2 mM O_2, whereas the wild-type K_i for O_2 is 300 μM. These results suggest that the region around Ser-368 controls access of O_2 to the enediol(ate) or that the seryl β-hydroxyl directly influences enediol(ate) reactivity. (ORNL is managed by Martin Marietta Energy Systems, Inc., under Contract DE-AC05-84OR21400 with the USDOE.)

51. Epitope Mapping of *E. coli* Pyruvate Dehydrogenase Complex and the E1 Decarboxylating Enzyme Using a Library of Monoclonal Antibodies. *Frank Jordan* and Alan McNally. Department of Chemistry, Rutgers University, Newark, NJ 07102. Lars Mattsson. Pharmacia Biosensors, Piscataway, NJ 08854.

A library of 21 monoclonal antibodies is reported to *E. coli* K12 pyruvate dehydrogenase complex (PDHc) and its E1 (thiamin-dependent, pyruvate-decarboxylating) subenzyme, 10 being produced by injecting the complex and 11 by injecting pure E1. Nearly all are IgG1 isotypes, 13 of them are found to bind both PDHc and E1, while 8 are bound only to PDHc. Inhibitory activities vis-a-vis PDHc ranged from 0 to as high as 98% within 1 min of mixing. Six monoclones elicited by PDHc and E1 each were further studied, indicating binding constants in the range $3–8 \times 10^9$ M^{-1}. The best inhibitory monoclone was shown to bind two antibodies/E1 dimer. In addition, competitive binding studies using radiolabeled E1 showed that the monoclones are directed to at least two different epitopes. The technique of surface plasmon resonance was used to further map the epitopes of both PDHc and E1, revealing that the three strongly inhibitory monoclones bind to the same region of E1. In addition, several monoclones appear to be binding noncontinuous epitopes. The strongly inhibitory monoclone should be a useful probe of the thiamin diphosphate binding locus as well as of the E1–E2 interaction locus through epitope mapping approaches. (Support of this research by Hoffmann-La Roche, Nutley, NJ, and NSF is gratefully acknowledged.)

52. High-Affinity Variants of Human Growth Hormone Obtained by Monovalent Phage Display. *H. B. Lowman* and J. A. Wells. Department of Protein Engineering, Genentech, Inc., 460 Point San Bruno Boulevard, South San Francisco, CA 94080.

We have used monovalent display of human growth hormone (hGH) mutants in the form of hGH-gene3 fusions on bacteriophage M13 for selection of hGH variants which bind with improved affinity to the cloned extracellular domain (hGHbp) of the hGH receptor [Lowman, H. B., et al. (1991) *Biochemistry 30*, 10832–10838]. Variants were assayed by competitive displacement of labeled hormone from hGHbp. A tight-binding variant from a helix 1 library binds 3.3-fold tighter than wild-type hGH. By successive rounds of mutagenesis on helix 4, we obtained a variant which binds about 8.3-fold tighter. Our experience with recruitment of hGHbp-binding determinants into nonbinding homologues of hGH indicated that the effects of enhanced binding may be additive for amino acid substitutions in different regions of the hGH molecule. By combining the highest affinity mutants previously obtained, we have produced an even tighter binding variant of hGH (K_d = 13 pM). However, some combinations of mutations are clearly nonadditive, and we have explored additional strategies, to be presented here, for sorting high-affinity hormone variants from partially-random "combinatorial" libraries of hGH.

53. Enhanced Substrate Specificity Observed in *Eco*RI DNA Methyltransferase upon Mutagenesis of Cysteine 223. *Karen Maegley* and N. O. Reich. University of California, Department of Chemistry, Santa Barbara, CA 93106.

The *Eco*RI DNA methyltransferase is part of a type-II restriction-modification system and methylates the second adenine in the recognition sequence GAATTC. Cys^{223} was implicated as a critical residue by our previous protein chemical data [(1990) *J. Biol. Chem. 265*, 17713–17719] and by homology to other DNA methyltransferases. Substitution of Cys^{223} with Ser, Ala, and Gly by site-directed methods produced three mutant enzymes, all with altered substrate specificity. Kinetic analysis of the mutant enzymes yields K_{cat} and K_{mDNA} values for the canonical site that do not significantly differ from those of the wild-type enzyme. However, a significant decrease in the methylation of noncanonical sequences is observed with the mutant enzymes both in vitro and in vivo. Our results suggest that either Cys^{223} is near the DNA binding region or that flexibility in the region of Cys^{223} may be important for specificity.

54. Cloning of a *Pseudomonas fluorescens* Gene Encoding for a Putative *p*-Hydroxybenzoate Hydroxylase Isozyme. *Barry M. Shuman*[1] and Thomas A. Dix.[1,2] Departments of [1]Chemistry and [2]Biological Chemistry, University of California, Irvine, CA 92717.

A PCR amplification was performed on *P. fluorescens* genomic DNA with the intention of isolating a portion of the gene that encodes for the flavoprotein *p*-hydroxybenzoate hydroxylase (PHBH). This yielded an 850-bp fragment (expected size) whose DNA sequence coded for a protein having close homology to the published [Weijer, W. J., et al. (1983) *Eur. J. Biochem. 133*, 109] PHBH amino acid sequence. A radiolabeled probe was prepared using this fragment to screen a *P. fluorescens* library constructed in λgt11. Several positives were isolated whose DNA coded for a 394 amino acid protein (the size of PHBH); a 75% homology to the published amino acid sequence was determined. This homology, coupled with the fact that all the residues essential for binding flavin and substrate are present, suggests that a gene coding for a PHBH isozyme has been isolated. The gene is being subcloned behind the T7 promoter and will be expressed to enable evaluation of the protein's catalytic activity.

55. Synthesis of Fluorogenic and Chromogenic Substrates for the Sensitive Detection of β-Lactamase and Mutants. *Daniel L. Woodard*, Patrick D. Mize, J. Michael Quante, Randal A. Hoke, O. Elmo Millner, and Paul T. Hamilton. Becton Dickinson Research Center, 21 Davis Drive, Research Triangle Park, NC 27709.

New fluorogenic and chromogenic substrates for the detection of β-lactamase and related mutant enzymes are described. Desacetyl cephalothin and desacetyl cefotaximine are linked to either 7-amino-4-methylcoumarin (AMC) or 3-aminoindole through an *O*-carbamoyl tether and thus serve as substrates for these enzymes. Upon cleavage of the cepham ring by β-lactamase, an electron cascade results in the release of the fluorophore or chromophore. In the case of the AMC-containing substrate, the released moiety can be detected by fluorescence (ex 365 nm/em 440 nm). The released 3-aminoindole can be detected by the use of diazonium salts which couple to the indole ring and result in colored precipitates. The rates of hydrolysis for the fluorogenic substrates are compared for several mutant enzymes which are found in antibiotic-resistant strains of bacteria.

56. Advantages of Using Multiple Sequence Alignments over Pairwise Alignments When Sequence Similarity Is Low. *P. C. Babbitt*, D. Dunaway-Mariano, and G. L. Kenyon. University of California, San Francisco, CA 94143, and University of Maryland, College Park, MD 20742.

Alignment of multiple sequences can reveal patterns suggestive of primary sequence relationships that are missed by pairwise alignment strategies. We show, for example, striking similarities between a recently obtained sequence of one component of 4-chlorobenzoate dehalogenase and 13 other protein sequences. Some of these patterns were missed by pairwise alignment algorithms. This alignment can also be used to illustrate the pitfalls of determining the significance of relationship or lack thereof by percent identity calculations. Multiple alignment of these 14 sequences produced lower percent identities between sequences than did pairwise alignments of the same sequences. We suggest that this was due to removal of "noise" generated by the matching of random residues in pairwise alignments. Thus, sequences in the alignment discussed above were clearly related even though the overall percent identities between many of the pairs fall below 10%. (Supported by USPHS Grants GM28688, AR17323, and GM40570.)

57. The Cyclophilin Multigene Family of Peptidyl–Prolyl Isomerases: Characterization of Three Separate Human Isoforms. *M. J. Bossard*, M. Brandt, D. J. Bergsma, T. G. Porter, and M. A. Levy. SmithKline Beecham Pharmaceuticals, Box 1539, King of Prussia, PA 19406.

Cyclophilin (CyP), a major cytosolic protein possessing peptidyl–prolyl cis–trans isomerase (PPIase) activity, has been implicated as the specific receptor of the immunosuppressive drug cyclosporin A (CsA). However, its abundance and broad tissue distribution argue against it having a specific role mediating the action of CsA in T cells. To identify other potential CsA receptors related to CyP, a human cDNA library was screened. Two cDNAs were identified that encode distinct proteins related to human hCYP1. Each hCyP protein was cloned, expressed, purified, and shown to be an active PPIase. Substrate specificity was examined with 11 synthetic peptides (Suc-Xaa-Yaa-Pro-Phe-4-nitroanalide), and inhibition of the PPIase activities associated with hCyP1, hCyP2, and hCyP3 was studied with CsA, MeAla^{6}CsA, and MeBm$_2$t^1-CsA. These results are discussed with regard to therapeutic relevance.

58. Alternate and Minimal Catalytic Motifs for Proteolysis by Trypsin. *David R. Corey* and Charles S. Craik. Department of Pharamceutical Chemistry, University of California, San Francisco, San Francisco, CA 94143.

The catalytic triad of serine proteases, Asp-His-Ser, is one of the classic motifs of enzymology. Effective strategies for the incorporation of the triad into non-protease protein scaffolds (i.e., antibodies or de novo designed peptides) might allow the development of sequence-specific peptidases. Such catalyst design would be facilitated by knowledge of the limits within which the orientation or composition of the triad members can be altered while still preserving significant peptidase activity. Our approach to this has been twofold: (1) to determine the minimum catalytic amino acids required and (2) to examine catalysis by alternate configurations. These experiments demonstrate that an intact catalytic triad is not a requirement for peptide bond cleavage, and suggest that designed serine peptidases need not include a catalytic histidine or aspartic acid. In addition, high levels of activity can be maintained if the catalytic aspartic acid at position 102 is removed and its function is replaced by an introduced aspartic or glutamic acid at position 214.

59. Examining Hydrophobic Hydration Shells with FTIR Spectroscopy. *David Hecht*, Lema Tadesse, and Lee Walters. Department of Molecular Biology, The Scripps Research Institute, La Jolla, CA 92037.

Systematic differences exist in the vibrational transitions of water molecules that are associated with the hydration shells surrounding various hydrocarbon-containing solutes (such as amino acids and alkylsulfonates) in aqueous solution. As the surface area of the hydrocarbon moiety of the solute is increased, there are corresponding changes in the vibrational intensities and frequencies of the solvating water molecules. These changes indicate an increase in the number of hydrogen bonds present in the solute-induced hydration shell. These observations are consistent with previous theories which postulate that hydration shells become progressively more structured and thermodynamically stable as the "hydrophobicity" of the dissolved solute increases.

60. Hinged "Lid" Motion of the Triosephosphate Isomerase Loop. *D. Joseph-McCarthy*,[1,2] G. A. Petsko,[3] and M. Karplus.[2] [1]Department of Chemistry, Massachusetts Institute of Technology, Cambridge, MA 02139, [2]Department of Chemistry, Harvard University, Cambridge, MA 02138, and [3]Rosenstiel Basic Medical Sciences Research Center, Brandeis University, Waltham, MA 02254.

Triosephosphate isomerase (TIM) is used as a model system to study how a localized conformational change in a protein structure is produced and related to enzyme reactivity. TIM has an 11-residue loop region that moves more than 7 Å and closes over the active site when substrate binds. The loop acts like a "lid" in that it moves rigidly and is attached by two hinges to the remainder of the protein. Results of molecular dynamics calculations confirm the structural analysis and suggest a possible ligand-induced mechanism for loop closure. Calculations that determine a possible reaction path for the loop transition from the closed to the open conformation are presented.

61. Structural Studies of a Prototypic Helix Peptide by ^{1}H NMR. *Frank Mari*, Minzhen Xu, Robert E. Humphreys, and George E. Wright. Department of Pharmacology, University of Massachusetts Medical Center, Worcester, MA 01655.

Prototypic helix peptide PH-1.0 (LYQELQKLTQTLK) has a maximal hydrophobic strip thought to regulate scavenging of T cell-presented peptides during antigen processing and the nucleation of α-helices in proteins [(1990) *J. Immunol. 145*, 899; (1991) *J. Biol. Chem. 266*, 5521; (1991) *Ibid. 266*, 10054]. CD studies showed that PH-1.0 and a series of analogues systematically changing Leu→Thr in the longitudinal hydrophobic strip were equally α-helical in trifluoroethanol (TFE)–water, but only those with strong hydrophobic strips were helical on lipid vesicles. High-resolution ^{1}H NMR studies were undertaken to obtain detailed information on the segmental structure of PH-1.0. Solvent and temperature related changes in peptide NH chemical shifts and NH–αCH coupling constants reflected an increasing degree of ordered structure with increased TFE concentrations and at low temperatures. Two-dimensional techniques (TOCSY and NOESY) were applied to make sequence-specific assignments of proton resonances in water and in TFE–water mixtures. Interresidue crosspeaks derived from NOESY experiments are consistent with increased helical content of PH-1.0 in TFE–water. (Supported in part by ACS-IM-582 and NIH RR05649.)

62. Stabilization of α Helical Structures in Short Peptides. Behrouz Forood, Eva J. Feliciano, and *Krishnan P. Nambiar*. Department of Chemistry, University of California, Davis, CA 95616.

Several peptides were designed and synthesized to study the α helix stabilizing effect of hydrogen bonds between NH groups at the amino termini and CO groups at the carboxy termini of α helices that are not part of intrahelical hydrogen bonds with side-chain functional groups of amino acids external to the helices. The best helix inducers are peptides that contain Asp-Pro at the amino terminus which allow hydrogen bonding between the carboxylic acid side chain of Asp and two free NH groups at the amino terminus and having an Arg at the carboxy terminus whose side chain can hydrogen bond with two free carbonyls at the carboxy terminus of the α helix. Our results also provide experimental proof for such a hypothesis put forth by Jane Richardson and G. D. Rose by comparing the sequences of several proteins whose X-ray structures have been determined.

63. Magnetic Resonance Spectroscopic Investigation of Phase Transitions in Dehydrated and Hydrated Mammalian Stratum Corneum. *S. J. Rehfeld*,[1] U. Simonis,[2] and W. Z. Plachy.[2] [1]Department of Dermatology, University of California, San Francisco, CA 94143, and [2]Department of Chemistry and Biochemistry, San Francisco State University, San Francisco, CA 94132.

The stratum corneum (SC), the outermost component of the epidermis, serves as a barrier to water as well as many chemicals. The SC is a multiphasic system composed primarily of corneocytes (protein and some lipids) embedded in a lamellar bilayer structure composed predominantly of lipids. This unique structure of the SC is responsible for permeability of some chemicals. An understanding on a molecular level of the function of phase transitions in SC observed by differential scanning calorimetry would be extremely useful. To further define the role of both lipid and protein in controlling water loss and chemical permeability, we employed both proton magnetic resonance (^{1}H NMR) and electron paramagnetic resonance (EPR) spectroscopy. The EPR spin probe used was ^{13}C depleted perdeuterated di-*tert*-dibutylnitroxide, pdDTBN. Analysis of ^{1}H NMR and EPR spectra of mammalian stratum corneum as a function of temperature and hydration revealed specific phase transitions associated with acyl chain melting, and dehydration and rehydration associated with the sphingolipids and glycosphingolipids. All transitions occurred between ≈5 and 50 °C.

64. Enhanced Hydrophobic Binding of Pertussis Toxin in the Presence of Oligosaccharide Receptor Analogues. *Brenda D. Spangler*,[1] Louis D. Heerze,[2] and Glen D. Armstrong.[2] [1]Biological and Medical Research Division, Argonne National Laboratory, Argonne, IL 60439, and [2]Department of Medical Microbiology and Infectious Diseases, University of Alberta, Edmonton, Alberta, Canada T6G 2H7.

Pertussis toxin (PT) is one of several virulence factors produced by the bacterium *Bordetella pertussis*, the causative agent of whooping cough. Using size-exclusion HPLC, we found that when PT was mixed with specific glycoprotein receptor analogues, both components of the mixture disappeared from solution in a time-dependent and concentration-dependent manner. PT–biotin and biotinylated glycoproteins used as probes indicated that complexation with these glycoproteins greatly enhanced the ability of PT to adsorb to hydrophobic surfaces. We propose that the increased hydrophobicity may enhance the association of the toxin with the plasma membrane of host cells and, possibly, trigger delivery of the enzymatic subunit, S1, to the intracellular compartment.

65. Synthesis and Chemical Modification of the Peptide Analogues of the Acetylcholine Receptor Binding Region of Neurotoxins. *Noel S. Sturm*, Christopher Schwarz, and Richard A. Hudson. University of Toledo, Department of Medicinal and Biological Chemistry, College of Pharmacy, and Department of Chemistry, 2801 West Bancroft, Toledo, OH 43606.

Our long-standing interest in the molecular basis for the action of the curarimimetic neurotoxins (Tsernoglou et al., 1978) and, in particular, the molecular identity of the interacting surfaces within the complex formed between these toxins and the nicotinic acetylcholine receptor (AcChR) led us to the

synthesis and evaluation of several model peptides designed to mimic central loop structure and geometry of the neurotoxin. Early crystallographic analyses of toxin structure (Tsernoglou & Petsko, 1976; Low et al., 1976) led us to propose that a cluster of amino acid residues located at the tip of an extended β-sheet were intimately involved in AcChR binding (Tsernoglou et al., 1978). To determine the importance of particular residues believed to be involved in binding to the AcChR, a number of peptides were synthesized. We describe the synthesis, purification, and receptor binding activity of the peptides. (This work was partially supported by Grant NIH-NINCDS-NS22851.)

66. Quantifying Secondary Structure at a Specific Residue: FTIR Spectroscopy of Isotopically Labeled Peptides. *Lema Tadesse*, David Hecht, Ramina Nazarbaghi, and Lee Walters. Department of Molecular Biology, The Scripps Research Institute, La Jolla, CA 92037.

A method for examining secondary structure at specific sites in conformationally heterogeneous peptides in aqueous solution has been established. Isotopic substitution of individual residues in peptides makes it possible to determine the conformation of a single residue at a specific site. Quantitative information about populations present in α-helical and random coil conformations can be obtained from spectral peak areas so that equilibrium constants can be calculated for the recruitment of a single residue into an α-helical conformation.

67. Folding of *trp* Repressor Fragments into a Native-like Assembly. *M. L. Tasayco*, K. Valentine, and J. Carey. Department of Chemistry, Princeton University, Princeton, NJ 08544.

The unique dimeric architecture of the *trp* aporepressor of *E. coli* (TrpR) built from two highly intertwined chains implies that subunit dimerization is a step on the folding pathway. Despite the complexity of both the architecture and folding kinetics of TrpR, its reversible two-state folding precludes the structural characterization of its folding intermediates. Proteolytic cleavage of each subunit at positions 7 and 71 provides the N and C fragments (residues 8–71 and 72–108, respectively), separating the hydrophobic core into subdomains. Biochemical and biophysical characterization of the purified fragments indicate a native-like dimeric assembly of N fragments and a rather unstructured C fragment. Interestingly, an equimolar mixture of N and C fragments produces an NMR spectrum essentially indistinguishable from that of the intact protein, indicating a native-like dimeric assembly of TrpR fragments. Thus, the results of this proteolytic approach support folding via partially folded dimeric intermediates and, furthermore, illuminates the hierarchy of subdomain folding in TrpR.

68. Inorganic Phosphate Binding to Chicken Erythrocyte H4 Histone Protein. Michael J. Minch and *Hai Minh Vu*. Department of Chemistry, University of the Pacific, Stockton, CA 95211.

The binding of ^{32}P-phosphate to purified H4 protein was studied by equilibrium partitioning studies across 3000-kDa molecular weight selective semipermeable membrane in an Amicon micropartition system. Linear Scatchard plots were obtained indicating two specific binding sites and dissociation constants in the millimolar range. NMR methods were also employed. ^{31}P NMR line widths were measured as a function of added histone H4 protein or with the 23 amino acid N-terminal peptide fragment of H4. The line widths increased markedly in the presence of protein or peptide. The binding to peptide was shown to be pH dependent with the binding increasing upon deprotonation of the peptide His-18 residue. There are also significant changes in the histone ^{1}H NMR spectrum upon binding to inorganic phosphate.

69. Calculation of Transformed Thermodynamic Properties of Biochemical Reactants at Specified pH AND pMg. *Robert A. Alberty*. Department of Chemistry, Massachusetts Institute of Technology, Cambridge, MA 02139.

The fundamental equation of thermodynamics for the transformed Gibbs energy G' at specified pH and pMg is used to derive the expressions for the standard transformed Gibbs energy of formation $\Delta_fG'^\circ$(i) of a reactant, its standard transformed enthalpy of formation $\Delta_fH'^\circ$(i), and its standard transformed entropy of formation $\Delta_fS'^\circ$(i). The standard transformed Gibbs energy of reaction $\Delta_rG'^\circ$, standard transformed enthalpy of reaction $\Delta_rH'^\circ$, and standard transformed entropy of reaction $\Delta_rS'^\circ$ can be written as functions of pH and pMg in terms of the standard Gibbs energies of formation Δ_fG°(i), standard enthalpies of formation Δ_fH°(i), and standard entropies of formation Δ_fS°(i) of the species involved. These expressions can be rearranged to the usual forms involving a reference reaction. The standard transformed formation properties are calculated for glucose 6-phosphate (G6P) at 298.15 K, 1 bar, pH = 7, pMg = 3, and I = 0.25 M.

70. Solvent Isotope Partitioning: Measurement of Desorption Rates of Reactant Water from Binary and Ternary Enzyme–Substrate Complexes in Proteases. *Thelma S. Angeles*, Gerald A. Roberts, Steven A. Carr, and Thomas D. Meek. Departments of Medicinal Chemistry and Physical & Structural Chemistry, SmithKline Beecham Pharmaceuticals, King of Prussia, PA 19406.

The hydrolases are unique among bireactant enzymes in that one of their substrates, H_2O, is also the reaction solvent. Accordingly, the role of H_2O in the kinetic mechanisms of these enzymes is refractory to direct investigation, the hydrolases are treated as unireactant enzymes, and the rates of binding and desorption of water from the binary enzyme–H_2O and enzyme–H_2O–substrate complexes remain uncharacterized for these enzymes. To study these kinetics, we have adapted the isotope partitioning method of Rose et al. [(1974) *J. Biol. Chem. 249*, 5163] to determine the rates of desorption of H_2O from the enzyme–H_2O–(substrate) complexes of the proteases, porcine pepsin, and thermolysin, by "solvent" isotope partitioning, wherein the binary enzyme–$H_2{}^{18}O$ complex established in the "pulse" solution is diluted into a large pool of $H_2{}^{16}O$ upon rapid mixing with a "chase" solution composed of variable substrate concentrations. The extent of trapping of $H_2{}^{18}O$ within the respective E–$H_2{}^{18}O$ and E–$H_2{}^{18}O$–substrate complexes was determined from mass spectrometric analysis of the hydrolytic products.

71. Inactivation of Cystathionine β-Synthase by Difluoroalanine. *D. R. Arnelle* and R. H. Abeles. Graduate Department of Biochemistry, Brandeis University, Waltham, MA 02254.

Cystathionine β-synthase is a PLP-dependent enzyme catalyzing the formation of cystathionine from serine [or monofluoroalanine (MFA)] and homocysteine. Slow exchange between the α-protons of serine or MFA and solvent is observed in the absence of the second substrate. No pyruvate

formation has been observed from either substrate. In the presence of D,L-difluoroalanine (DFA), the enzyme partitions between fluoropyruvate production and inactivation. The enzyme is inactivated with K_i = 10 μM, k_{inact} = 0.7 min^{-1} at pH 7.8; extensive dialysis vs buffer containing PLP does not restore catalytic activity. One inactivation event occurs for every three turnovers. Both serine and homocysteine protect against DFA inactivation. A mechanism whereby binding to the second substrate induces a rotation about the C2–C3 of the first substrate has been invoked to account for these data.

72. Spectroscopic Observation of the Kinetic Fate of a Thiamin-Bound Enamine Intermediate in Water. *Gabriel L. Barletta* and Frank Jordan. Department of Chemistry, Rutgers University, Newark, NJ 07102.

Earlier we reported spectroscopic observation of enamines (2-α-carbanion), structurally related to the key intermediate in all thiamin diphosphate (TDP) dependent enzymatic pathways [see Jordan, F., et al. (1987) *J. Am. Chem. Soc. 109*, 4415; Barletta, G., et al. (1990) *J. Am. Chem. Soc. 112*, 8144]. Evidence was presented in Me_2SO for the delocalized nature of the carbanion, the pK_a leading to it from thiazolium salts, as well as for their facile one-electron electrochemical oxidation. We have succeeded at generating and analyzing the rate of buildup and disappearance of the enamine in water for the first time, using a stopped-flow instrument. Based on produced analysis and Hammett parameters obtained for the rate constants, we propose this mechanism to explain our observations:

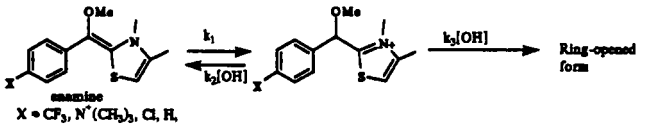

The individual rate constants as well as the pK's for the reaction leading to the enamine of some of the analogues studied were calculated using the ϵ for the enamine obtained in nonaqueous medium. The uncertainties in the interpretation of the nonaqueous data having been lifted, we can estimate for the first time: (a) the enzyme-induced lowering of the pK shown in the eq and (b) the catalytic rate acceleration provided by the enzymes for k_2. (Supported by NIH/MBRS and NSF.)

73. Regulation of Pyruvate Decarboxylase Reflected in the Kinetic Behavior of Enzyme-Bound Intermediates. *Jose Buenaseda*, Xiaoping Zeng, and Frank Jordan. Department of Chemistry, Rutgers, The State University, Newark, NJ 07102.

It was recently reported that the thiamin diphosphate-dependent enzyme pyruvate decarboxylase (PDC) when exposed to the substrate analogues of the formula X-C_6H_4CH=$CHCOCO_2H$ will convert them to two different products on decarboxylation: X-C_6H_4CH=$CHCHO$ (the anticipated product) and the product of apparent misprotonation X-$C_6H_4CH_2CH_2CO_2H$ (followed by tautomerization) of the enamine intermediate [Zeng et al. (1991) *J. Am. Chem. Soc. 113*, 5842]. The ratio of the two products, as well as the rate of formation of the enamine intermediate monitored at 440 nm, was dependent on the presence of the allosteric regulator pyruvamide. We now report results on the kinetics and inhibition patterns resulting from X = $BrCH_2$, FCH_2. For X = $BrCH_2$ the enamine eliminates bromide ion forming a quinone methide that can also be monitored at 570 nm and whose formation rate is dramatically affected by the regulator. For X = FCH_2, the ratio of dihydrocinnamic acid to cinnamaldehyde product is decreased severalfold on addition of pyruvamide. (Supported by the NSF (DMB), the NIH-MBRS (B. Komisaruk, PI) and the Rutgers Busch Fund.)

74. UV-Light Induced Photocleavage of 6-Phosphogluconate Dehydrogenase from *Torula* Yeast by Vanadate Tetramer. Thomas J. Zamborelli, Robert S. Brown, and *Debbie C. Crans*. Department of Chemistry, Colorado State University, Fort Collins, CO 80523.

Photolytically induced vanadate chemistry is used to probe the active site of 6-phosphogluconate dehydrogenase. 6-Phosphogluconate dehydrogenase is inhibited by vanadate in a competitive inhibition pattern with respect to 6-phosphogluconate. The inhibiting species was previously identified using a combination of enzyme kinetics and ^{51}V NMR spectroscopy as the vanadate tetramer ($V_4O_{12}^{4-}$). The ability of the vanadate tetramer to associate tightly (K_i 0.013 μM) with proteins is somewhat curious considering the high charge of the tetramer; characterizations of the tetramer binding site were therefore explored. Photolysis of the 6-phosphogluconate dehydrogenase from *Torula* yeast in the presence of vanadate generated two cleavage products, the major product at 51 kDa and the minor product at 46 kDa. Enzyme activity measurements were correlated with the cleavage and found to correlate with the major cleavage product. The cleavage site of the subunit corresponding to the major product appears to be located at the binding site of the substrate. We employed matrix-assisted laser desorption (MALD) mass spectrometry to observe both the high and low molecular weight cleavage products. The biological implications of our findings are discussed.

75. Imidazoleglycerol-3-phosphate Synthase: A Glutamine Amidotransferase in Histidine Biosynthesis. Thomas J. Klem and *V. Jo Davisson*. Department of Medicinal Chemistry and Pharmacognosy, Purdue University, West Lafayette, IN 47907.

The *hisH* gene of *E. coli* encodes a protein that bears significant amino acid sequence homology with the general class of *trpG*-type glutamine amidotransferases. Our studies have focused on establishing a catalytic function for this protein in the histidine biosynthetic pathway which is in part responsible for the conversion of N^1-(5′-phosphoribulosyl)formimino-5-aminoimidazole-4-carboxamide ribonucleotide (PRFAR) to 5′-(5-aminoimidazole-4-carboxamide) ribonucleotide (AICAR) and imidazole glycerol-3-phosphate (IG-3-P). For this purpose, we have over expressed all of the constituent *E. coli* histidine biosynthetic genes and have purified the proteins encoded by the *hisA*, *hisH*, and *hisF* genes. Studies with the purified proteins indicate that the *hisH* protein has no inherent glutamine amidotransferase, glutaminase, or IG-3-P synthase activity. However, in combination with the *hisF* protein, all three of these enzymatic properties are displayed. Gel filtration studies indicate that the *hisH* and *hisF* proteins form a dimeric species that has the full catalytic capacity for the conversion of PRFAR to IG-3-P and AICAR without the production of a diffusable intermediate. Current research involves a kinetic investigation of this multistep enzyme reaction and further physical analysis of the dimeric protein complex.

76. On the Catalytic Mechanism of an Enzyme-Mediated Amadori Rearrangement. Susan E. Hamilton, Ina Lim, and *V. Jo Davisson*. Department of Medicinal Chemistry and

Pharmacognosy, Purdue University, West Lafayette, IN 47907.

Despite the presence of several unusual and unique catalytic transformations in the histidine pathway, the enzymes have not been characterized. The reaction catalyzed by the enzyme N^1-(5′-phosphoribosyl)formimino-5-aminoimidazole-4-carboxamide ribonucleotide (5′-ProFAR) isomerase is formally an intramolecular redox process that is presumed to occur via a 1,2 prototropic shift known as an Amadori rearrangement. Although no studies of the enzymatic version of this process have been reported, this transformation is similar to that catalyzed by the ketose/aldose isomerases. An overexpression system for this enzyme has been developed in *E. coli* that has aided in its isolation and characterization. From amino acid sequence alignments, affinity labeling studies, and site-directed mutational analysis, a conserved histidine residue has been identified as an important feature of the catalytic mechanism of this enzyme.

77. Quantum Mechanical Interpretation of Experimental FTIR Carbonyl Frequency Shifts and Their Role in Catalysis by Triosephosphate Isomerase. *J. D. Evanseck* and M. Karplus. Department of Chemistry, Harvard University, Cambridge, MA 02138.

Quantum mechanical calculations of vibrational spectra have been used to elucidate the catalytic mechanism of triosephosphate isomerase (TIM) on the isomerization of dihydroxyacetone phosphate (DHAP) to D-glyceraldehyde 3-phosphate (D-GAP). Ab initio Hartree–Fock and semiempirical AM1 calculations for model compounds are used to examine the contribution of active site residues (Asn-10, Lys-12, His-95, Ser-96, Glu-97, and Glu-165) to the vibrational frequency shift observed for the carbonyl group of DHAP. X-ray crystal structures of phosphoglycolohydroxamate (PGH) complexed with wild-type TIM and the mutants H95Q and E165D were employed for the computations. Cooperativity between Lys-12 and Glu-165 and a salt-bridge involving Lys-12 and Glu-97 are two major interactions which significantly alter the induced polarization of DHAP. The absence of a carbonyl frequency shift in the H95Q and H95N mutants appears to be due to rearrangement of the active site, rather than being a direct effect of removing the histidine. Furthermore, the Glu-165 residue provides the largest carbonyl polarization of the residues examined, yet the effects from Lys-12, His-95, and Glu-97 can not be ignored. The protein backbone of Ser-96 and Glu-97, and the phosphate group of DHAP have no apparent influence on DHAP carbonyl polarization.

78. Magnetic Field Effects on the Photolytic Decomposition of Methylcob(III)alamin. *Charles B. Grissom*, Alexander M. Chagovetz, and Zhaolin Wang. Department of Chemistry, University of Utah, Salt Lake City, UT 84112.

The rate of anaerobic photolysis of methylcob(III)alamin by steady-state UV irradiation to produce cob(II)alamin and $^{\bullet}CH_3$ as a geminate radical-pair is decreased 2.5-fold in the range 400–600 G. A magnetic field effect is only seen in highly viscous media (i.e., 20% Ficoll 400 $\eta/\eta_0 = 30$) that reinforce radical-pair recombination. At magnetic fields greater than 1500 G (where the Δg mechanism of singlet–triplet intersystem crossing becomes significant), the rate of photolysis is increased. This suggests the radical-pair is formed in the singlet state. Since only radical-pair reactions are affected by an exogenous magnetic field, the observed results are direct evidence of homolytic Co–C bond cleavage.

79. L-683,845, a Potent and Specific Monocyclic β-Lactam Inhibitor of Human PMN Elastase. *B. G. Green*, R. Chabin, D. Kuo, H. Weston, J. Doherty, C. Dorn, P. Finke, W. Hagmann, J. Hale, M. MacCoss, S. Shah, and W. B. Knight. Departments of Enzymology and Medicinal Chemistry, Merck, Sharp and Dohme Research Laboratories, Rahway, NJ 07065.

L-683,845, [*S*-(*R**,*S**)]-4-[(1-(((1-(5-benzofuranyl)butyl)amino)carbonyl)-3,3-diethyl-4-oxo-2-azetidinyl)oxy]-benzeneacetic acid is a potent, mechanism based inhibitor of human PMN elastase (PMNE). L-683,845 inactivated PMNE with $k_{inact}/K_i = 8.5 \times 10^5$ M^{-1} s^{-1}, which was 3-fold less potent than α_1P_I ($k_{inact}/K_i = 2.2 \times 10^6$ M^{-1} s^{-1}). The individual kinetic constants for the inhibition by L-683,845 at pH 7.5 were $k_{inact} = 0.06$ s^{-1} and $K_i = 0.06$ mM. Inactivation was efficient since it required only 1.7 equiv of inhibitor, but this is indicative of some partitioning between turnover of inhibitor and inactivation. The β-lactam was an efficient inhibitor of the elastase-catalyzed solubilization of elastin. L-683,845 displayed greater activity versus human and primate PMN elastases than versus the enzyme from rat or dog. Human chymotrypsin and cathepsin-G were weakly inhibited by L-683,845 ($k_{inact}/K_i = 14$ and 40 M^{-1} s^{-1}, respectively). The compound did not inhibit other proteases or esterases. L-683,845 produces a stable E–I complex that slowly reactivated releasing several products ($t_{1/2} = 7$ h at 37 °C). Boiling the E–I complex produces a characteristic substituted urea stoichiometrically. Since the production of this urea is mechanism based, it can be used as a diagnostic in a clinical setting.

80. Sulfate Anion Alters the Arrangement of Substrates Bound at the Active Site of Yeast Phosphoglycerate Kinase (PGK). *Jay D. Gregory* and Engin H. Serpersu. Department of Biochemistry, University of Tennessee, Knoxville, TN 37996-0840.

β,γ-Bidentate $Cr(H_2O)_4ATP$ (CrATP) was used as a paramagnetic NMR probe of the active site geometry of PGK. The paramagnetic effect of CrATP on the longitudinal relaxation rates of 3-PGA protons revealed longer metal–proton distances in the presence of activator sulfate. Computer models which satisfy the observed distances show significant alteration in the arrangement of the substrates at the active site. NMR studies of the paramagnetic effect of CrATP on water protons upon titration of 3-phosphoglycerate (3-PGA) into the binary CrATP·PGK complex exhibited complex behavior wherein enhancement was observed at low 3-PGA concentration, which decreased at higher 3-PGA concentration. Nearly opposite enhancement behavior was observed in the presence of sulfate ion, which is consistent with the altered environment of the metal when sulfate is present.

81. NMR Evidence of a Novel DNA-Dependent Mutase Activity Associated with Yeast Phosphoglycerate Kinase. *Jay D. Gregory* and Engin H. Serpersu. Department of Biochemistry, University of Tennessee, Knoxville, TN 37996-0840.

An enzymatic activity of intramolecular transfer of the phosphoryl group from C3 to C1 of 3-phosphoglycerate (3-PGA) in the absence of Mg^{2+}-ATP was found to be associated with yeast PGK isolated from yeast strain 20B-12 containing multicopy plasmid pCGY219. The presence of DNA was shown to be required for the activity. ^{31}P NMR spectrum showed the appearance of a new resonance in the phosphorous

spectrum of 3-PGA, whose chemical shift is identical to that observed for the 1-phosphoryl of 1,3-diphosphoglycerate. The increase in intensity of this new peak with time is accompanied by a corresponding decrease in the intensity of the 3-phosphoryl resonance. Similarly, ^{1}H NMR showed a simultaneous simplification in the splitting pattern of the C3 protons consistent with the loss of a phosphoryl group from C3.

82. Isolation of Lysozyme from Nurse Shark Serum. *A. Hedayati*, B. A. Warden, and S. L. Smith. Department of Medical and Laboratory Sciences, Florida International University, Miami, FL 33199.

The purpose of this study was to isolate lysozyme from nurse shark (a primitive elasmobranch) serum. To isolate the lysozyme from other serum proteins, heparin affinity and gel filtration chromatography were used. Evaluation of the purity of the isolated fraction was performed by means of SDS–PAGE electrophoresis. A faint band, which required further purification, was observed at a molecular weight of approximately 14000. The lysozyme activity of the chromatographic fractions was determined by the lysoplate and turbidimetric methods, using *Micrococcus lysodeicticus* as the substrate and hen egg white lysozyme as the standard. Nurse shark lysozyme exhibited optimal activity under the following conditions: (1) temperature = 37 °C, (2) substrate concentration = 0.2 mg/mL, and (3) pH = 6.2.

83. Electrospray Ionization Mass Spectrometry as a Mechanistic Tool: Elucidation of the Structure of Covalent E–I Complexes of Human Leukocyte Elastase and Cathepsin-G. *W. B. Knight*,[1] K. Swiderek,[2] J. Calacay,[1] J. Shively,[2] T. Lee,[2] T. Sakuma,[3] B. Shushan,[3] and R. Mumford.[1] [1]Department of Enzymology, Merck Sharp & Dohme Research Labs, Rahway, NJ 07065, [2]Division of Immunology, City of Hope, Duarte, CA, and [3]Sciex Instruments, Thornhill, Canada.

We have utilized electrospray ionization mass spectrometry to probe the nature of covalent E–I complexes of human leukocyte elastase (HLE) and cathepsin-G (Cat-G). The mass spectrum of HLE isozyme-4 displayed a major component with a mass of approximately 25 200 amu. Inactivation of HLE with 3-(acetoxymethyl)-7α-methoxy-8-oxo-5-thia-1-azabicyclo[4.2.0]oct-2-ene-2-(2-(*S*)-carboxypyrrolidinecarboxamide) 5,5-dioxide increased the mass by 357 amu. This indicates that the acetyl group was liberated from the exocyclic methylene. Inactivation of HLE with *trans*-4-ethoxycarbonyl-3-ethyl-1-[(4-nitrophenyl)sulfonyl]azetidin-3-one increased the mass by that of the parent compound. This observation demonstrates that HLE does not catalyze a β elimination of *p*-nitrophenylsulfonate as Firestone et al. [(1990) *Tetrahedron 46*, 2255] suggested. In addition, it suggests that a "double hit" of both the active site serine and histidine residues is not required to form a stable acyl enzyme. The mass spectrum of Cat-G isozyme 3 was complex, but the spectrum was shifted by approximately 500 amu upon reaction with Succ-AAPF-CMK. This indicates that the chloride was not present in the Cat-G–I complex and is consistent with displacement of the chloride by the active site histidine to produce the stable complex. These data demonstrate that mass spectrometry can be used to probe the mechanism of inhibition of enzymes by mechanism-based inhibitors that produce stable E–I complexes.

84. NMR Docking of the Inhibitor 3′,5′-pdTp into the X-ray Structure of Staphylococcal Nuclease (SN). *D. J. Weber*, E. H. Serpersu, A. G. Gittis, E. E. Lattman, and A. S. Mildvan. Johns Hopkins School of Medicine, Baltimore, MD 21205.

In the X-ray structure of the ternary SN–Ca^{2+}–3′,5′-pdTp complex, the conformation of pdTp is distorted by Lys-70 and Lys-71 from an adjacent molecule of SN [(1989) *Proteins: Struct., Funct., Genet. 5*, 183]. In solution this problem does not occur. Based on eight Co^{2+}–nucleus distances from paramagnetic effects on T_1 and 10 interproton distances from 1D and 2D NOE studies, the conformation of enzyme-bound metal–pdTp in solution is low anti ($\chi = 18 \pm 3°$) with a C2′-endo/O1′-endo sugar pucker ($\delta = 142 \pm 1°$) trans, gauche about the C4′–C5′ bond ($\gamma = 310 \pm 19°$), and anticlinal about the C3′–O3′ bond ($\epsilon = 274 \pm 4°$). The structure of pdTp in the crystal differs, with a high anti conformation ($\chi = 40°$) and a gauche, trans orientation about C4′–C5′ ($\gamma = 186°$). The undistorted solution conformation of enzyme-bound metal–pdTp was docked into the X-ray structure of SN by superimposing the metals and using 12 intermolecular NOEs from ring protons of Tyr-85, Tyr-113, and Tyr-115 to protons of pdTp. The 5′-phosphate of the docked NMR structure of pdTp overlaps with that of the X-ray structure and interacts similarly with Arg-35 and Arg-87. However, the 3′-phosphate, sugar, and thymidine are significantly displaced from their positions in the X-ray structure.

85. Mechanism of Substrate Recognition of Class A β-Lactamases. Glenn Zafaralla, Elias Manavathu, Stephen Lerner, and *Shahriar Mobashery*. Department of Chemistry, Wayne State University, Detroit, MI 48503.

β-Lactamase-promoted fragmentation of penicillins and cephalosporins is the principal microbial activity which confers resistance to the β-lactam antibiotics. A detailed knowledge of interactions of β-lactamase and substrates is indispensable to the understanding of how these enzymes function and evolve. The highly conserved arginine-244 has been postulated to play a role in the initial recognition of substrates by class A β-lactamases; however, in the final enzyme–substrate complex no direct function has been attributed to this residue. Studies of the purified wild-type TEM-1 and Arg-244-Ser mutant β-lactamase attributed apparent binding energies of 1.3–2.3 kcal/mol for the penicillins, and 0.3–1.0 kcal/mol for the cephalosporins to the transition-state and ground-state species by arginine-244. These results were interpreted to indicate the involvement of a long hydrogen bond between arginine-244 and the substrate carboxylate, both in the ground and transition states. A reassessed picture for substrate anchoring within the active site, involving coordination of the side chains of Arg-244, Ser-130, and Ser/Thr-235 to the substrate carboxylate, is proposed to accommodate these observations. For a carbapenem antibiotic bound in the active site in this manner, one N_η of the Arg-244 guanidinium moiety approaches to within 2.5–3 Å of the σ framework of the pyrroline double bond of the antibiotic. Accordingly, both kinetic and graphics evidence will be presented which indicate that Arg-244 facilitates the characteristic $\Delta^2 \rightarrow \Delta^1$ pyrroline tautomerization of carbapenems in the course of turnover—a process which accounts for the inhibitory properties of carbapenems toward β-lactamases. The details of graphics analysis of β-lactamase, computer-assisted rational design of point-mutant enzymes, mechanism of active site anchoring of the substrates, and the critical influence of Arg-244 in the turnover processes will be presented.

86. Hydrogen-Deuterium Exchange in Pyridoxol. Possible Participation of 3-OH. *B. Paul* and W. Korytnyk. Grace Cancer Drug Center, Roswell Park Cancer Institute, Buffalo, NY 14263.

Pyridoxol (I) when heated with hydrazine-d_4 was converted

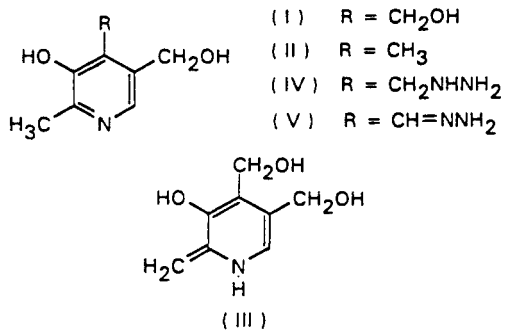

to 4-deoxypyridoxol (II; 4-DOP) where hydrogens at 2-CH_3, 4-CH_3, and 6-H were exchanged by deuterium; whereas under similar conditions no exchange was observed in γ-collidine [Korytnyk & Ahrens (1971) *J. Med. Chem. 14*, 947]. Our studies on the mechanism show that hydrogens at 2-CH_3 in I are exchanged by deuterium when heated in D_2O, indicating the formation of an enamine-typed intermediate (III). The formation of 4-CD_3 from 4-CH_2OH probably involves the initial formation of pyridoxylhydrazine (IV) and its conversion to pyridoxalhydrazone (V) in four steps. By hydrogen abstraction and N_2 elimination V is converted to II. (Supported by Grants CA-13038 and CA-08793 from the National Cancer Institute.)

87. The Effect of Unsaturated Bonds in the Acyl Chains of Phospholipids. *Linda L. Pearce* and Stephen C. Harvey. The University of Alabama at Birmingham, Department of Biochemistry, Schools of Medicine/Dentistry, UAB Station, Birmingham, AL 35294.

Historically it has been difficult to study lipid membranes as they function at temperatures well-above the phase transition temperatures and are therefore much more disordered than in the crystal state. Biological membranes participate in numerous biological functions, and the majority of these functions appear to be critically dependent on the types of lipids comprising the membranes. Recently the use of computer simulations to study biological membranes has brought great insight into their molecular motion. We present a molecular dynamics study of the effect of the incorporation of unsaturated bonds into a simulation of the acyl chains of phospholipids and complete results with those obtained using NMR spectroscopy.

88. Mechanistic Aspects of N-Linked Glycosylation. Barbara Imperiali, *Keith W. Rickert*, Karen L. Shannon, and Masafumi Unno. Department of Chemistry, California Institute of Technology 164-30, Pasadena, CA 91125.

N-Linked glycosylation, an important step in eukaryotic protein processing, involves a glycosidic link of an oligosaccharide to the normally unreactive asparagine side-chain amide nitrogen. Previous studies have shown the importance of the conformation of the peptide substrate in allowing glycosylation. Based on this, we have formulated a mechanism to explain the enhanced nitrogen nucleophilicity. Several peptides containing various asparagine analogues have been synthesized and are examined for their ability to act as substrate and/or compete with substrate, allowing us to examine those structural and electronic properties of asparagine important for enzyme recognition and turnover.

89. Kinetics of Metal Stimulation and Inhibition in CTP Synthetase. *James G. Robertson* and Joseph J. Villafranca. Department of Chemistry, The Pennsylvania State University, University Park, PA 16802.

Apo-CTP synthetase was prepared by dialysis against 5 mM EDTA. Apoenzyme contained no detectable amounts of Mg^{2+}, Mn^{2+}, Cu^{2+}, Zn^{2+}, Co^{2+}, Ni^{2+}, Fe^{2+}, or bound EDTA. The half-saturation value for Mg^{2+}-dependent enzyme activation was ≈2 mM at a total concentration of 2 mM nucleotides. This result suggests that the enzyme requires more Mg^{2+} than required simply to complex the nucleotide substrates. Apoenzyme also was activated by Mn^{2+} and Co^{2+}. The half-saturation values for Mn^{2+} and Co^{2+} were ≈0.5 and ≈1.0 mM, respectively. Over the range of 0.1 to 10 mM, neither Cu^{2+}, Zn^{2+}, Ni^{2+}, nor Ca^{2+} activated the enzyme. Under conditions where nucleotide substrates were complexed 1:1 with Mg^{2+}, addition of Mn^{2+} or Co^{2+} stimulated the enzyme. This result is consistent with the presence of a separate metal binding site on the enzyme. In addition, both Cu^{2+} and Zn^{2+} were effective inhibitors of CTP synthetase in the absence of dithiothreitol at concentrations <50 μM. Inhibition by Zn^{2+} was reversible by EDTA, whereas inhibition by Cu^{2+} was not. In the presence of dithiothreitol, Zn^{2+}, Co^{2+}, and Ni^{2+} inhibited the enzyme at less than 200 μM metal. In steady-state inhibition experiments, Zn^{2+} and Cu^{2+} demonstrated noncompetitive inhibition with respect to free Mg^{2+}, where K_{is} and K_{ii} were 0.3 and 0.8 μM for Zn^{2+} and 18 and 80 μM for Cu^{2+}.

90. Crystallization and Characterization of a *Candida rugosa* Lipase. *Byron Rubin*,[1] Miroslaw Cygler,[2] Penny Smith,[1] Yunge Li,[2] and David Harrison.[1] [1]Eastman Kodak Company, Rochester, NY 14650, and [2]Biotechnology Research Institute, National Research Council of Canada, Montreal, Canada H4P 2R2.

A neutral lipase isolated from the fungus *Candida rugosa* has been crystallized and a molecular replacement solution has been achieved. Of the several lipases present in *Candida*, the enzyme with lipolytic activity, having an isoelectric point of 4.2, was crystallized from 2-methyl-2,4-pentanediol in MES buffer in the presence of calcium (II) salts. The crystal symmetry is $C222_1$ with cell dimensions a = 64.9 (1) Å, b = 97.2 (1) Å, and c = 175.8 (2) Å and with one 61 000 M_r molecule in the asymmetric unit. The protein shows high sequence and structure homology to lipase isolated from *Geotrichum candidum* and a high degree of sequence homology to pancreatic cholesterol ester hydrolase. Particularly conserved in the three sequences are those residues flanking the active site serine. In addition the two disulfide bonds in the proteins also appear to be conserved. The structure was solved using both real space and reciprocal space rotation/translation techniques and is being refined using a combination or molecular dynamics and constrained least squares refinement. At the present 2.8-Å resolution, some ambiguities in the chain tracing exist. Diffraction is strong to 2-Å resolution, and work is underway to extend the resolution and continue the refinement of the model.

91. Role of Internal Thermodynamics in Determining the Extent of Hydrogen Tunneling for Enzyme Catalyzed Hydride and Proton Transfer Reactions. *J. Rucker*, Y. Cha, T. Jonsson, and J. P. Klinman. Department of Chemistry, University of California, Berkeley, CA 94720.

Previous studies from this laboratory have demonstrated the importance of room temperature hydrogen tunneling in enzyme-catalyzed hydride and proton transfer reactions. Theoretical treatments of hydrogen tunneling indicate an increase

in the probability of tunneling as the equilibrium constant for H transfer approaches unity. Given the ability of enzymes to perturb internal equilibrium constants toward unity, tunneling may arise more frequently at enzyme active sites than in solution. Using bovine plasma amine oxidase and yeast alcohol dehydrogenase to study proton and hydride tunneling, respectively, we have shown that tunneling remains significant as substrate structures are altered relative to parent compounds. An analysis of internal thermodynamics in the yeast alcohol dehydrogenase reaction indicates (i) that $\Delta H°$ is endothermic for benzyl alcohol to benzaldehyde interconversions and (ii) that $\Delta H°$ deceases in proceeding from electron-withdrawing to electron-releasing ring substitutents. Concomitant with the decrease in internal $\Delta H°$ values, the role of hydrogen tunneling increases. These studies provide support for the view that internal thermodynamics will influence tunneling at enzyme active sites. (Supported by the National Science Foundation).

92. Structural and Mechanistic Studies on *E. coli* β-Hydroxydecanoyl Thiol Ester Dehydrase. Barry S. Henderson, James R. Gillig, and *John M. Schwab*. Department of Medicinal Chemistry and Pharmacognosy, Purdue University, West Lafayette, IN 47907.

E. coli β-hydroxydecanoyl thiol ester dehydrase, which catalyzes a key step in the biosynthesis of unsaturated fatty acids, equilibrates thiol esters of (*R*)-3-hydroxydecanoic acid, (*E*)-2-decenoic acid, and (*Z*)-3-decenoic acid. Dehydrase is susceptible to mechanism-based inactivation by the substrate analog 3-decynoyl-NAC (an *N*-acetylcysteamine thiol ester). Dehydrase is also inactivated by 1-diazo-4-undecyn-2-one (DUO), by a mechanism that parallels inactivation of de-

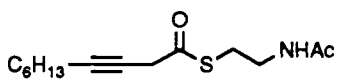

3-decynoyl-NAC

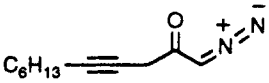

DUO

hydrase by 3-decynoyl-NAC. Photoirradiation of the initial adduct leads to Wolff rearrangement of the diazoketone. Studies designed to elucidate the fate of the resulting ketene will be presented. A collaborative effort is also underway to determine the three-dimensional structure of dehydrase by X-ray crystallography. Studies directed toward the synthesis of a 3-decynoyl-NAC analogue that will enable the incorporation of a heavy atom into the derivatized protein will also be described.

93. Stereochemical Course of the Reaction Catalyzed by *E. coli* Imidazoleglycerol-Phosphate Dehydratase. Jeffrey A. Moore, Aulma R. Parker, V. Jo Davisson, and *John M. Schwab*. Department of Medicinal Chemistry and Pharmacognosy, Purdue University, West Lafayette, IN 47907.

Imidazoleglycerol-phosphate (IGP) dehydratase catalyzes the mechanistically-cryptic conversion of IGP to imidazoleacetol phosphate (IAP). As one aspect of the complete characterization of the enzyme's structure and catalytic mechanism, the stereochemical course of the reaction is under investigation. Efficient expression systems for the *E. coli* enzymes IGP dehydratase and IAP transaminase have been constructed, and I[3-^{2}H]GP has been synthesized by a coupled, enzymatic route, beginning with chemically-synthesized [3-^{2}H]ribose-5-phosphate. Labeled IGP is converted by the dehydratase to IAP, and then immediately to histidinol, by the combined action of IAP transaminase and histidinol phosphatase. ^{1}H NMR spectroscopy is used to compare the

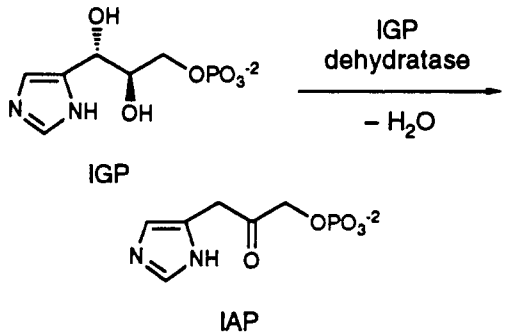

enzymically-derived, chirally-labeled histidinol to a synthetic standard.

94. Solvent Isotope Effects on Retinal Cis–Trans Isomerization in the Dark Adaptation of Bacteriorhodopsin. *Stanley Seltzer*. Chemistry Department, Brookhaven National Laboratory, Upton, NY 11973.

The solvent isotope effect on the first-order rate constant for dark adaption of bacteriorhodopsin, near neutral pH (pD) is inverse: $k_D/k_H = 1.24$, suggesting that proton movement in the rate-controlling step is unlikely. The fit of the isotope effect's dependence on the atom fraction of deuterium in the solvent to the Gross–Butler equation leads to the conclusion that the proton(s) in motion is(are) less tightly bound in the reactant than in a reactive intermediate formed prior to the rate-controlling step of cis–trans isomerization. The near-unity isotope effect on the equilibrium between bound 13-*cis*- and *all-trans*-retinals in the dark-adapted state mixture indicates that the isotope effects on the forward and reverse rate constants for isomerization are approximately equal to each other and equal to the isotope effect on the observed rate constant for dark adaptation. The results support a previously proposed mechanism of rate-controlling Asp-212 nucleophilic catalysis of retinal cis–trans isomerization in the dark adaptation process. (Research supported by U.S. Dept. of Energy, Division of Chemical Sciences.)

95. Structural and Kinetic Characterization of Vanadate-Derived Amino Acid Complexes by ^{1}H, ^{13}C, and ^{51}V NMR. Part 1: Structure. *Paul K. Shin* and Debbie C. Crans. Department of Chemistry, Colorado State University, Fort Collins, CO 80523.

Vanadate reacts with multidentate ligands to form complexes ligated by both nitrogen and oxygen moieties. Depending on the structure of the ligand, the vanadium center can be either pentacoordinate or hexacoordinate. Potentiometric analysis and ^{51}V NMR show that vanadate forms 1:1 complexes with diethanolamine (DEA) and *N*-[tris(hydroxymethyl)methyl]glycine (Tricine). *N*,*N*-Bis(2-hydroxyethyl)-glycine (Bicine) and *N*-(2-hydroxyethyl)iminodiacetic acid (HIDA) also complex vanadium(V). However, for these ligands, two distinct types of 1:1 complexes are observed depending on the solution pH. Both tridentate and tetradentate ligation are suggested by ^{1}H, ^{13}C, and ^{51}V NMR data for these complexes. The extent of ligation is determined by the number and type of potential binding moieties and pH. The coordination environment is also dependent upon these factors. *N*-(2-Hydroxyethyl)ethylenediamine triacetic acid (HEDT) also forms two pH-dependent vanadate complexes. One complex (low pH) is similar to that formed with EDTA, whereas the other (high pH) is more similar to the vanadate complexes with bicine and HIDA. These results indicate the preferential formation of a five- or six-coordinate vanadium

complex depending on the number and type of ligating moieties in amino acid derivatives.

96. GC/MS Studies of Nitrogen Flow in Cyanophycin Metabolism in *Synechococcus PCC6308*. Margaret V. Merritt, Mary M. Allen, Ludmila Mesh, and *Silvia S. Sid*. Departments of Chemistry and Biological Sciences, Wellesley College, Wellesley, MA 02181.

Cyanophycin (multi-L-arginyl-poly[L-aspartic acid] or CGP) is a nitrogen storage peptide in most cyanobacteria; its concentration decreases under conditions of nitrogen limitation and increases immediately on restoration of a nitrogen source. GC/MS studies of the *N*-trifluoroacetyl, *n*-butyl ester (TAB) derivatives of the amino acids from hydrolyzed CGP have been used to monitor the nitrogen incorporation into CGP from ^{15}N-labeled substrates under various growth conditions. CGP is isolated from ruptured cells via acid extraction; additional purification steps included extraction with hexane/isopropanol (3/2) to remove lipids interfering with the formation and/or stability of the TAB derivatives. Our experiments indicate that nitrogen-starved cells rapidly incorporate ^{15}N into CGP upon repletion of the media with ^{15}N-nitrate; uniform labeling of the nitrogens in CGP-derived aspartic acid and arginine was observed within 6 h of nitrogen repletion. At shorter times following repletion, the ^{15}N content (the guanido nitrogens of arginine) was significantly lower than the other arginine nitrogen and that of aspartic acid.

97. Methylenetetrahydrofolate Reductase: Not a Two-Faced Mechanism. *James S. Sumner* and Rowena G. Matthews. Department of Biological Chemistry, The University of Michigan, Ann Arbor, MI 48109.

Methylenetetrahydrofolate reductase, a flavoprotein, catalyzes the NADPH-linked reduction of 5,10-methylenetetrahydrofolate, CH_2FH_4, to 5-methyltetrahydrofolate, CH_3FH_4, committing the tetrahydrofolate-bound one carbon unit to the regeneration of the methyl group of methionine. In our studies FAD was replaced with 8-demethyl-8-hydroxy-5-deaza-5-carba-FAD, 8OH5DFAD, on the enzyme. This flavin analogue does not stabilize a one-electron-reduced species and may be reduced stereospecifically to *si*- or *re*-[5-^{3}H]8OHFADH$_2$. Reoxidation of *si*-[5-^{3}H]8OHFADH$_2$ with CH_2FH_4 or NADP shows direct tritium transfer to CH_3FH_4 and NADPH whereas reoxidation of *re*-[5-^{3}H]8OHFADH$_2$ leads to retention of tritium in the oxidized flavin. Thus, both substrates interact on the si side of the flavin ring, consistent with the observed ping-pong kinetics. The NADPH–CH_2FH_4 activity of apoenzyme incubated with 8OH5DFAD was shown to be approximately half of the activity when apoenzyme was incubated with FAD. These experiments have demonstrated a catalytically competent mechanism in which a hydride equivalent is transferred from NADPH to CH_3FH_4 through the si side of 8OH5DFAD. (Supported in part by GM 24908 from the National Institutes of Health.)

98. Construction of a Mechanism-Based Inhibitor for *Eco*RI DNA Methyltransferase. *Kim R. Sweetnam* and Norbert O. Reich. Chemistry Department, University of California, Santa Barbara, CA 93106.

Our results using *N*-ethylmaleimide modification suggest that cysteine 223 is critical for the *Eco*RI DNA methyltransferase catalyzed methylation of the second adenine in the GAATTC recognition sequence. A plausible catalytic mechanism involving this cysteine is shown below:

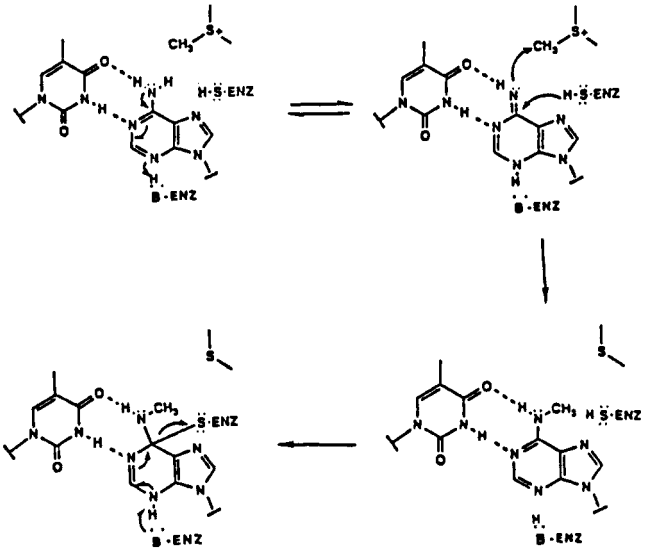

A key feature is the formation of a methylase-DNA covalent intermediate. We are testing this mechanism by incorporating a 6-chloropurine riboside into the DNA substrate. This substituted analogue is proposed to act as a mechanism-based or active site directed inactivator due to the excellent leaving group potential of the 6-chloro moiety. We are submitting this analogue to inactivation analysis and isolating the peptide sequence attached to the DNA to determine the reactive residue in the catalytic site of *Eco*RI DNA methyltransferase.

99. Differences in Substrate Specificities of Monoamine Oxidase A from Human Liver and Placenta. *A. K. Tan*, W. Weyler, J. I. Salach, and T. P. Singer. Department of Biochemistry and Biophysics, University of California, San Francisco, CA 94143, and Molecular Biology Division, Department of Veterans Affairs Medical Center, San Francisco, CA 94121.

Monoamine oxidase (MAO) type A from human placenta has been available in nearly homogeneous form for several years. More recently, catalytically active MAO A from human liver has been expressed in mammalian cells in culture and in *Saccharomyces cerevisiae* and has now been obtained in highly purified form from the latter source by modifications of the procedure previously used for isolation of the placental enzyme. The availability of novel substrates which are rapidly oxidized by MAO A from placenta and of new and potent competitive inhibitors of the enzyme provided an opportunity to compare the substrate specificities and affinities for competitive inhibitors of MAO A from two different tissues of the same species. This study demonstrates that while the K_m values for a series of natural and synthetic substrates are the same or nearly the same for the enzyme from these two tissues, significant differences in turnover numbers have been found, particularly with respect to bulky tetrahydropyridine derivatives.

100. Stereospecific Ketonization of 2-Hydroxymuconate. *Christian P. Whitman*, Robert J. Watson, William H. Johnson, and Michael E. Bembenek. College of Pharmacy, The University of Texas, Austin, TX 78712.

Groups of enzymes whose individual members subject similar substrates to identical chemical reactions are common in microbial degradative pathways. One such group includes 4-oxalocrotonate tautomerase (4-OT), 5-carboxymethyl-2-hydroxymuconate isomerase (CHMI), and 2-hydroxyhepta-2,4-diene-1,7-dioate isomerase (HHDDI) which catalyze the

ketonization of 2-hydroxymuconate (**1**), 5-carboxymethyl-2-hydroxymuconate (**2**), and 2-hydroxyhepta-2,4-diene-1,7-dioate (**3**), respectively, to their α,β-unsaturated ketones. The three enzymes have been isolated and found to be very different proteins. Despite these differences, CHMI and HHDDI ketonize **1** to 2-oxo-3-*trans*-hexenedioate (**4**), although at a considerably slower rate than that observed for 4-OT. In order to explore the extent to which the active sites of these three enzymes are related, the stereospecificity of 4-OT, CHMI, and HHDDI utilizing **1** in ^2H_2O was determined. The product, 5-[^{2}H]-**4**, was trapped and processed to 2-[^{2}H]glutaric acid by chemical degradative procedures. The configuration of the glutaric acid was established by comparison to an authentic sample. All three enzymes ketonize **1** stereospecifically to (*S*)-5-[^{2}H]-**4**. This result suggests that the active sites of 4-OT, CHMI, and HHDDI are more closely related than their structures indicate.

101. Oxygen Activation in Dopamine β-Hydroxylase. *Gaochao Tian*, Joe Berry, and Judith P. Klinman. Department of Chemistry, University of California, Berkeley, CA 94720, and Department of Plant Biology, Carnegie Institution of Washington, Stanford, CA 94305.

Considerable experimental evidence exists for the generation of a substrate-derived benzylic radical in the H-abstraction reaction catalyzed by dopamine β-hydroxylase. By contrast, the hydroxylating species responsible for benzylic radical formation has been uncertain. Isotopic methods and variation of transition-state structure have been used to address this question. Apparent oxygen isotope effects with H- and D-substrates and apparent deuterium isotope effect have been determined for five phenethylamine derivatives. The intrinsic oxygen isotope effect on the reaction, calculated by using the three experimental isotope effects, is found to decrease from 1.0281 to 1.0256, 1.0236, 1.0215, and 1.0216 as the rate of the H-abstraction step decreases from 680 to 500, 145, 22, and 2 s^{-1}, respectively. In all cases the intrinsic oxygen isotope effects, which are the product of the equilibrium isotope effect on formation of the hydroxylating species and the kinetic isotope effect on the H-abstraction, are larger than measured values for O_2 binding to hemoglobin, hemerythrin, and hemocyanin. The trends in isotope effects as a function of changing substrate reactivity show that bound oxygen must be cleaved prior to H-abstraction, ruling out superoxy or peroxy species as the hydroxylating agent. (Supported by a grant from the National Institutes of Health.)

102. Cancer Detection: Characteristics of B-Protein Production. *E. T. Bucovaz*, J. C. Morrison, and W. D. Whybrew. Department of Biochemistry, University of Tennessee—Memphis, Memphis, TN 38163.

Individuals with cancer have a protein in their serum which is named B-protein. Because of the close correlation of B-protein serum levels with the state of the malignancy, there is considerable interest in its investigation. It was determined that B-protein is not specific for cancer although the protein was present in the serum of 87% of 2670 patients tested with the disease. Pregnancy and severe tissue damage also cause an elevation in serum B-protein levels. Both cancer-induced B-protein and pregnancy-induced B-protein have been purified and their characteristics have been compared. Although both B-proteins were similar in molecular weight, dimeric properties, carbohydrate content, p*I*, electrophoretic mobility, Sephacryl S-200 patterns, and binding to WGL-Sepharose and protein A-agarose, they differed in amino acid composition and binding to Affi-Gel Blue. Based on these studies it would appear that cancer-induced B-protein and pregnancy-induced B-protein are not homogeneous.

103. Excretion of 11-Dehydrothromboxane B_2: A Quantitative Index of TXA_2 Formation in Human Circulation. *Aldo Ferretti* and Vincent P. Flanagan. Human Nutrition Research Center, USDA ARS, Beltsville, MD 20705.

Reliable data on urinary excretion of 11-dehydrothromboxane B_2 (11-DTX) in healthy humans are lacking. We determined base-line excretion levels in 24-h urine from 35 male volunteers (24–57 years of age) by gas chromatography–tandem mass spectrometry. Prior to urine collection the subjects have been on a controlled basal diet providing 40% of energy from fat with P/S ratio about 0.8:1 for 10 weeks [Ferretti et al. (1991) *Lipids 26*, 500–503]. The mean daily excretion of 11-DTX, determined over a 72-h period, was 825 ± 404 (SD) ng (range 68–2508 ng). We could not detect any significant correlation between 11-DTX excretion (an index of endogenous synthesis of the vasoconstrictor and platelet agonist thromboxane A_2) and age, body weight, BMI, or urine volume. Under base-line conditions, i.e., in the absence of pharmacological or dietary intervention, excretion of 11-DTX is another biological variable the magnitude of which is typical of each subject, like blood pressure and metabolic rate.

104. Protection of Erythrocytes by Riboflavin. Feng Xu and *Donald E. Hultquist*. Department of Biological Chemistry, The University of Michigan, Ann Arbor, MI 48109-0606.

An NADPH-dependent reduction of riboflavin to dihydroriboflavin is catalyzed by the erythrocyte enzyme, flavin reductase. This laboratory has recently isolated and studied bovine flavin reductase. We now report that this enzyme, in the presence of NADPH and riboflavin, catalyzes the reduction of ferryl myoglobin. Photochemically-generated dihydroriboflavin reacts directly and rapidly with ferryl myoglobin to form ferrous myoglobin, with horseradish peroxidase–H_2O_2 complex to form ferric peroxidase, and with the products of cytochrome *c* peroxidation to prevent bleaching and to form the ferrous derivative. This evidence that dihydroriboflavin reacts rapidly with the higher oxidation states of hemeproteins and with hydroxyl radical, together with our detection of flavin reductase in various cells, suggested that riboflavin would serve as an effective therapeutic agent to protect against reperfusion injury. Preliminary studies show that riboflavin does protect erythrocytes from damage as measured by cell lysis. The effectiveness of riboflavin in protecting isolated organs from reperfusion injury is now being tested in collaborative studies. (Supported in part by NIH Grant AG-07046.)

105. Effects of 2-Chloro-2′-deoxyadenosine Triphosphate Incorporation on the Rate of Primer Extension by Human DNA Polymerases α and β. *S. K. Chunduru*, J. R. Appleman, and R. L. Blakley. Department of Biochemical and Clinical Pharmacology, St. Jude Children's Research Hospital, Memphis, TN 38105.

2-Chloro-2′-deoxyadenosine triphosphate (CldATP) is a potent antileukemic agent that is incorporated into DNA inhibiting DNA synthesis. We measured the rates of incorporation of CldATP into DNA during primer extension by human DNA polymerases α and β on an M13mp18 template. Extension is limited to five or six bases by omitting one or two normal dNTP's. Products were separated by electrophoresis and the relative concentrations estimated by autoradiography

and densitometry for reaction times of 0–10 min. The rate constant for the addition of each nucleotide was calculated by fitting these data to the CRICF (Chemical Reaction Integrated Curve Fitting) program. For a section of template with the sequence (3′→5′): AAATT, rate constants for each successive nucleotide addition by DNA polymerase β in the presence of 100 μM dATP, and dTTP were 0.55 ± 0.02, 1.98 ± 0.10, 1.25 ± 0.06, 2.00 ± 0.12, and 2.31 ± 0.17 min^{-1}. Constants with a system containing 100 μM CldATP, dTTP by DNA polymerase β were 0.150 ± 0.005, 0.040 ± 0.004, and <0.001 min^{-1}. [Supported by American Lebanese Syrian Associated Charities and John H. Sununu Fellowship (S.K.C.).]

106. The Role of Nonspecific DNA in the Site-Location Kinetics of the *Eco*RI DNA Methyltransferase. *Mark A. Surby* and Norbert O. Reich. University of California, Chemistry Department, Santa Barbara, CA 93106.

The *Eco*RI DNA methyltransferase is an extremely efficient enzyme, with a k_{cat}/K_m of 4.1×10^8 s^{-1} M^{-1} for plasmid DNA. Its k_{cat}/K_m decreases to 0.51×10^8 s^{-1} M^{-1} when a 14-base-pair synthetic oligonucleotide is used as a substrate. Canonical site flanking sequence differences between the plasmid and the 14-bp oligonucleotide were shown to have no effect on k_{cat}/K_m. A possible explanation for these observations is that the methylase utilizes facilitated diffusion along nonspecific DNA as a mechanism for site location. This was first tested using a processivity assay developed for the *Eco*RI endonuclease [(1985) *J. Biol. Chem. 260* (24), 13130–13137]. In contrast to our results with the endonuclease, no processive methylation was observed with this assay. The role of facilitated diffusion in initial site location was then investigated by kinetic analysis of restriction fragments ranging in size from 4363 to 108 bp, all of which contained a single *Eco*RI site. There were no differences observed in the rate of methyl group incorporation for the various substrates. This leads us to conclude that the specificity enhancement observed for the plasmid DNA is due to nonspecific sequences <108 bp away from the canonical site of the DNA substrate.

107. Structural Predictions of Sequence Modified Analogues of d(GGCGGAATTCGCGG)·d(CCGCCTTAAGCGCC) Using Molecular Dynamics. *S. Falsafi*, and N. Reich. Department of Chemistry, University of California, Santa Barbara, CA 93117.

The object of this computational investigation is to determine the structural consequences of single base pair substitutions in the canonical site GAATTC of 14 base pair oligonucleotide duplexes. The computational schemes reported herein are guided by the earlier approaches established by Kollman and co-workers and include 200 ps of molecular dynamics calculation. The atomic trajectories are computed with the united atom force field of AMBER [(1986) *AMBER 3.0A*, UCSF] and the temporal variations of the backbone torsion angles and the helicoidal parameters are analyzed with the Dials and Windows [(1989) *J. Biomol. Struct. Dyn. 6*, 669] algorithms. We first performed two computations using the crystal structure of the Dickerson dodecamer and the standard Arnott B-DNA structure as the starting points. The torsion angles, α, β, γ, δ, ϵ, χ^1, χ^2, averaged over the entire simulation time show 3% difference between the two structures, suggesting convergence toward the global minimum. These results corroborate Kollman's earlier report [(1990) *Biopolymers 29*, 517–532], therefore establishing the validity of our approach. In view of our ongoing investigation with a series of 14 base pair oligonucleotides [(1991) *Biochemistry 30*, 2933–2939; *Nucleic Acids Res.*, in press], six sequence-modified analogues of d(GGCGGAATTCGCGG)·d(CCGCCTTAAGCGCC) were subjected to 200 ps of molecular dynamics. Additionally, in order to probe the behavior of low frequency structural fluctuations that appeared in the course of the 200-ps runs, one of the analogues was subjected to 1 ns of molecular dynamics. This report summarizes our findings within the context of purine–purine or purine–pyrimidine base pair generalizations in addition to base-pair-specific structural effects. Where appropriate, we discuss our results vis a vis those reported earlier on oligonucleotide structures in the solution and the crystalline states.

108. Binding of Pentaammineosmium(II) to Dimethyluracil and Uridine. *Karin A. Hughes*, Jason T. Call, and M. G. Finn. Department of Chemistry, University of Virginia, Charlottesville, VA 22901.

The pentaammineosmium(II) moiety has been shown to bind in an η^2-fashion to olefinic sites of pyrimidine bases. We will describe the formation of stable dihapto adducts of $(NH_3)_5Os^{2+}$ with dimethyluracil and uridine in both organic and aqueous solution. The presence of an excess of phosphate and carboxylate ions in the latter does not inhibit η^2 binding. Structural characterization of these small molecule complexes as well as the coordination of $(NH_3)_5Os^{2+}$ to calf thymus DNA will be described.

109. In Vitro and in Vivo Specificity Analysis of the *Eco*RI DNA Methyltransferase. *Norbert O. Reich*, Charlotte Olsen, Fabrizio Osti, John Murphy, Dean Smith, and Scott Crowder. Department of Chemistry, University of California, Santa Barbara, CA 93106.

The *Eco*RI DNA methyltransferase modifies the second adenine in the site GAATTC using the cofactor *S*-adenosylmethionine. We determined the in vitro sequence selectivity with a family of related hemimethylated 14mers (X = methyladenosine): top 5GGCG*GAATTC*GCGG3′/ 5CCGC*GAXTTC*CGCC3′ bottom. Comparisons of true k_{cat}, K_m^{DNA}, K_m^{AdoMet}, and k_{cat}/K_m^{DNA} show specificity decreases from 5- (GAATCC) to 23 000- (GGATTC) fold (top strand shown). For several substrates the decrease in k_{cat} makes a disproportionate contribution toward specificity, suggesting that discrimination is mediated by the placement of critical *catalytic* residues. Further evidence for this conclusion is provided by our observation that the stability of the methyltransferase–DNA complexes (determined by gel shift analysis) do not generally follow specificity changes. In contrast, no methylation of noncanonical sites was detectable in vivo. We used three assays to show that TAATTC, CAATTC, GTATTC, GGATTC, and GAGTTC are not methylated in vivo under conditions where the canonical site is protected. A possible reconciliation of these results with our in vitro data is that noncanonical methylation does occur in vivo but is actively repaired. The possible involvement of the recently identified *mrr* (methylated adenine recognition and repair) locus in this capacity is being investigated.

110. Preparation and Replication of Templates Containing Site-Specific Cis–Syn, Trans–Syn, (6–4), and Dewar Photoproducts of TpT. *C. A. Smith* and J.-S. Taylor. Department of Chemistry, Campus Box 1134, Washington University, St. Louis, MO 63130.

DNA templates, 49 nucleotides in length, containing site-specific cis–syn, trans–syn, (6–4), and Dewar photoproducts of TpT were prepared by the ligation of lesion-containing hexamers to flanking oligonucleotides. The (6–4) product-containing hexamer was prepared by 254-nm irradiation of d(AATTAA) and isolating the desired product by HPLC. The Dewar product-containing hexamer was prepared by 325-nm irradiation of the (6–4) product-containing hexamer. Both were characterized by high-field NMR. Decamers containing site-specific cis–syn and trans–syn dimers were prepared by automated DNA synthesis using photoproduct "building blocks". The 49-mers were characterized by chemical cleavage, exonuclease resistance, and polymerase blockage. The (6–4) photoproduct blocked all polymerases tried, but the cis–syn, trans–syn, and Dewar photoproducts could be bypassed by Sequenase Version 2.0, an exonuclease-free mutant of T7 DNA polymerase.

111. Interaction of a Tetrapeptide Containing Two Tryptophyl Residues with Nucleic Acids. *M. Vera*, C. Robledo-Luiggi, and I. D. Cruzado. Department of Chemistry, University of Puerto Rico, Mayagüez, Puerto Rico 00681.

The interaction of a tetrapeptide containing two tryptophyl residues, L-Lys-L-Trp-L-Ala-L-Trp, with nucleic acids was studied by NMR, fluorescence, viscosity, and T_m. Its interaction was compared to that of the tripeptide L-Lys-L-Trp-L-Lys and the tetrapeptide L-Lys-L-Ala-L-Ala-L-Trp. It was found that tryptophan's stacking interaction is favored by the presence of a second tryptophyl residue in the oligopeptide chain. Results also indicate that this tetrapeptide engages in bis-stacking interaction upon binding to DNA, in other words, both tryptophyl residues are stacked between the DNA bases, where the tryptophan in the second position seems to interact more than the one in the fourth position. Studies carried out with calf thymus DNA and polynucleotides will be presented. (Project funded by NIH/MBRS Grant SO6RR-08103.)

112. ^{13}C-Substituted Oligodeoxyribonucleotides: Synthesis and NMR Studies of CCAAT-Containing Single-Stranded Oligomers Related to the NF-I Binding Site in Adenovirus DNA Replication. *Jian Wu* and Anthony S. Serianni. Department of Chemistry and Biochemistry, University of Notre Dame, Notre Dame, IN 46556.

Structural studies of the initiation site for adenovirus DNA replication have been undertaken by examining the single-stranded octamer **1**, d(AGCCAATA), that comprises part of the NF-I recognition site. Two preparations of **1** were made using solid-state synthesis in which ^{13}C (99 atom %) was singly substituted at C-1′ of the A-1 and A-5 residues. High-resolution ^{13}C–^{1}H HMBC spectra (500 MHz) were obtained to selectively detect the furanose H-2′, H-3′, and H-4′ sites within the enriched residue, thereby assisting in their assignment in DQF-COSY spectra. The latter spectral data were supplemented by TOCSY and ROESY data to completely assign the ^{1}H NMR spectrum and to extract $^{3}J_{HH}$ values for furanose ring conformational analysis. Inspection of select DQF-COSY crosspeaks in the ^{13}C-substituted oligomers of **1** permitted the measurement of ^{13}C–^{1}H couplings of value in assessing local conformation. The chemical shifts and couplings observed in **1** have been compared to corresponding couplings in d(GCCAATA), d(CCAAT), d(ATA), and d(TA) to assess the effect of chain extension on preferred geometry. The use of selective ^{13}C labeling in the furanose component of oligomers should prove invaluable as this work is extended to larger portions of the NF-I binding site.

113. A Chemical Approach to the Single Site Cleavage of Human Chromosomes. *Peter B. Dervan.* Department of Chemistry, California Institute of Technology, Pasadena, CA 91125.

Pyrimidine oligonucleotides recognize purine sequences in the major groove of double helical DNA via triple helix formation. Specificity is imparted by Hoogsteen base pairing between the pyrimidine oligonucleotide and the purine strand of the Watson–Crick duplex DNA (TAT and C + GC base triplets). Due to the length of the recognition site (>16 base pairs), in a formal sense, this is 10^6 times more sequence specific than restriction enzymes and affords 65 536 new sequence specificities. The triple helix motif may be useful for single site cleavage of human chromosomes and the manipulation of sequence-specific protein–DNA binding. With regard to molecular recognition of double helical DNA by oligonucleotides, efforts to extend the triple helix motif to all four base pairs will be discussed.

114. Protein–Protein Recognition. *I. D. Kuntz*, B. Shoichet, and G. Bemis. Department of Pharmaceutical Chemistry, University of California, San Francisco, CA 94143-0446.

Our efforts at steric modeling of ligand–protein complexes have been extended to studies of macromolecular complexes. We show that the DOCK program can find intermolecular configurations that approximate the results of crystallographic studies of protease–protease inhibitor complexes, starting from the crystal structures of the proteins in isolation. Alternative orientations are also found. Extensions of this effort to other systems and other efforts at measuring molecular similarity will be described.

115. Crystal Structures of Protein–DNA Complexes: New Perspectives on Recognition and New Strategies for Design. *Carl O. Pabo.* Howard Hughes Medical Institute, Department of Biology, Massachusetts Institute of Technology, Cambridge, MA 02139.

We have determined the three-dimensional structures of a set of protein–DNA complexes, including representative examples from several major families of DNA-binding proteins. Comparing and contrasting these complexes (which include examples of the helix–turn–helix motif, the homeodomain, and the zinc finger) gives new perspectives on protein–DNA recognition and suggests new strategies for the design of novel DNA-binding proteins.

116. Mechanistic and Structural Studies on Cobalamin-Dependent Methionine Synthase from *Escherichia coli*. *Rowena G. Matthews*, James T. Drummond, Catherine L. Luschinky, and Martha Ludwig. Biophysics Research Division and Department of Biological Chemistry, The University of Michigan, Ann Arbor, MI 48109.

Cobalamin-dependent methionine synthase catalyzes the transfer of a methyl group from N^5-methyltetrahydrofolate to homocysteine, with the cobalamin prosthetic group serving as an intermediary in the methyl transfer. In contrast to other cobalamin-dependent enzymatic reactions, there is no evidence for radical chemistry in this reaction. Rather, the properties of cob(I)alamin as a supernucleophile appear to be exploited in the methionine synthase reaction, and both enzyme-bound cob(I)alamin and methylcobalamin are kinetically competent intermediates. We shall present recent studies on the inactivation of methionine synthase by nitrous oxide, a commonly used anesthetic. We have shown that nitrous oxide reacts with

enzyme-bound cob(I)alamin, and that the reaction liberates dinitrogen gas and involves the uptake of one proton. Our studies suggest that the enzyme catalyzes one electron reduction of N_2O, generating hydroxyl radical or its equivalent at the active site of the enzyme. We postulate that, most of the time, hydroxyl radical recombines harmlessly with enzyme-bound cob(II)alamin to form hydroxycob(III)alamin. However, occasionally, the hydroxyl radical escapes and inactivates the enzyme by reacting with the corrin prosthetic group or with residues at the active center. We shall also report on the progress toward determination of the structure of the cobalamin-binding domain of methionine synthase by X-ray crystallography.

117. Cloning and Sequencing of *Lactobacillus leichmannii* Ribonucleotide Reductase. *S. J. Booker* and J. Stubbe. Department of Chemistry and Biology, Massachusetts Institute of Technology, Cambridge, MA 02139.

Ribonucleotide reductases play an essential role in DNA biosynthesis providing the only mechanism for catalyzing the conversion of nucleotides to deoxynucleotides. It is quite intriguing, therefore, that the cofactors involved in this transformation have not been evolutionarily conserved. Reduction in aerobically grown *E. coli*, mammalian, and viral systems involves a diferric-tyrosyl radical cofactor. However, in *B. ammoniagenes* a "Mn" cofactor of unknown structure is involved, while an anaerobically grown *E. coli*, *S*-adenosyl methionine is involved. In *L. leichmannii* the cobalt cofactor, adenosyl cobalamin, is essential for nucleotide reduction. While neither the structure of the cofactors nor the quaternary structure of the proteins have been conserved, we have proposed that the chemistry of nucleotide reduction is very similar. In all cases it is postulated that the function of each cofactor is to initiate a radical dependent cleavage of the 3′ carbon–hydrogen bond of the nucleotide substrate. We would like to report the first sequence for a ribonucleotide reductase, not requiring iron, that of the B_{12}-dependent *L. leichmannii* protein. A comparison of this sequence with that of the B_1 subunit of the *E. coli* reductase will be examined in detail as will a comparison of the chemistry catalyzed by these two proteins.

118. Recent Progress in Vitamin B_{12} Biosynthesis. *A. Ian Scott*. Department of Chemistry, Texas A&M University, College Station, TX 77843-3255.

The acquisition of the enzymes for corrin biosynthesis through cloning and overexpression of the *cbi* genes from *Salmonella typhimurium* (with J. Roth) and the *cob* genes from *Pseudomonas denitrificans* (Crouzet et al.) has set the stage for the final assault on the complex problem of vitamin B_{12} biosynthesis. In this lecture, the recent results from Texas A&M will be reviewed and integrated with current research findings from other laboratories.

119. Genetic Approaches to the Synthesis and Physiological Significance of B_{12} in *Salmonella typhimurium*. *J. R. Roth*. Department of Biology, University of Utah, Salt Lake City, UT 84112.

In the bacterium *Salmonella typhimurium*, the biosynthetic genes for cobalamin are located in three separated regions of the genetic map. Most synthetic genes (approximately 20 of 25) are located in a single large operon whose expression is stimulated by cAMP and by a reduced cell interior; this operon is repressed by adenosyl-B_{12}. Nutritional requirements of mutants suggest that an early intermediate in corrinoid biosynthesis (prior to cobyric acid in the pathway) is adenosylated and that adenosyl cobinamide is an obligatory precursor to completion of cobalamin synthesis (addition of dimethyl benzimidazole). Only one gene has been associated with the ability to perform adenosylation in the de novo pathway; this gene is one of several alternatives needed to adenosylate exogenous corrinoids. One gene has been associated with ability to synthesize aminopropanol. *Salmonella* uses about 1% of its genome to encode the synthesis and transport of B_{12}. While this large genetic investment suggests an important physiological role for the cofactor, the four known B_{12}-dependent functions do not appear to be essential for growth of wild-type *Salmonella* under the laboratory conditions tested. It is particularly puzzling that *Salmonella* only synthesizes B_{12} when growing anaerobically.